THEORY AND PRACTICE OF CAVITY RF TEST SYSTEMS *

Tom Powers[†], Thomas Jefferson National Accelerator Facility

Abstract

Over the years Jefferson Lab staff members have performed about 2500 cold cavity tests on about 500 different superconducting cavities. Most of these cavities were later installed in 73 different cryomodules, which were used in three different accelerators. All of the cavities were tested in our vertical test area. About 25% of the cryomodules were tested in our cryomodule test facility and later commissioned in an accelerator. The remainder of the cryomodules were tested and commissioned after they were installed in their respective accelerator. This paper is an overview which should provide a practical background in the RF systems used to test the cavities as well as provide the mathematics necessary to convert the raw pulsed or continuous wave RF signals into useful information such as gradient, quality factor, RF-heat loads and loaded Q's. Additionally, I will provide the equations necessary for determining the measurement error associated with these values.

RF SOURCE

There are two fundamental ways to provide a low level RF (LLRF) drive signal to a cavity. In situations where beam is involved, fixed frequency RF systems are implemented. These make use of high gain phase and amplitude control loops. In these systems the mechanical length of the cavity is usually adjusted using tuners driven by motors, piezo crystals, or both. [1, 2, 3] Some systems make use of high power voltage controlled reactive tuners to pull the cavity's center frequency as seen at the fundamental power port.[4] An integral part of these LLRF systems is an interface to and algorithm for driving the tuner mechanism.

The second way is to make use of a LLRF system which is designed to track the cavity frequency. Such systems have two major advantages. They can be used with critically coupled SRF cavities, which have bandwidths on the order of 1 Hz, and the cavities do not need operational mechanical tuners. Thus, when there are pressure variations or frequency shifts due to microphonic or Lorentz effects, the LLRF system tracks the shifts and the cavity gradient is maximized for the given forward power and input coupling. Additionally, using such systems allows one to intentionally vary the cavity frequency so that the tuners can be fully characterized and measurements of phenomena such as dynamic Lorentz effects and microphonics can be studied [5]. The majority of the cavity tests completed at Jefferson Lab were done using voltage controlled oscillators configured in phase locked loops (VCO-PLL).

The VCO-PLL

A detailed mathematical treatment of phase locked loop circuits is provided in Reference [6]. The intent of this work is to go trough the practical considerations relating to VCO-PLLs when using them for driving superconducting cavities. Although these systems can be designed to be compact and inexpensive by using surface mount components and custom printed circuit boards, in most instances connectorized components are used in order to minimize the non-recurring design costs. All of the devices described are generally available in both formats.

Figure 1 shows a block diagram for a basic VCO-PLL The primary function of the low noise amplifier (LNA) and variable attenuators on the front end circuit is to ensure that the RF input to the mixer is not power starved or over driven. Additionally, they are used to adjust the loop gain, in order to avoid oscillations. LNAs with a noise figure between 1 and 3 dB are easily obtained and sufficient for this application. Thumbwheel switch controlled attenuators or PIN attenuators are frequently used. For all of these devices the phase shift of the device must be accounted for in the software or adjusted out as a course of normal operation.

Regarding loop gain, one needs to remember that the loop gain is proportional to cavity gradient. Thus a system that is stable when operated at 2 MV/m may be unstable when operated at 20 MV/m unless the loop gain is reduced at the higher gradients. In a number of systems we have found that replacing the LNA with a limiting
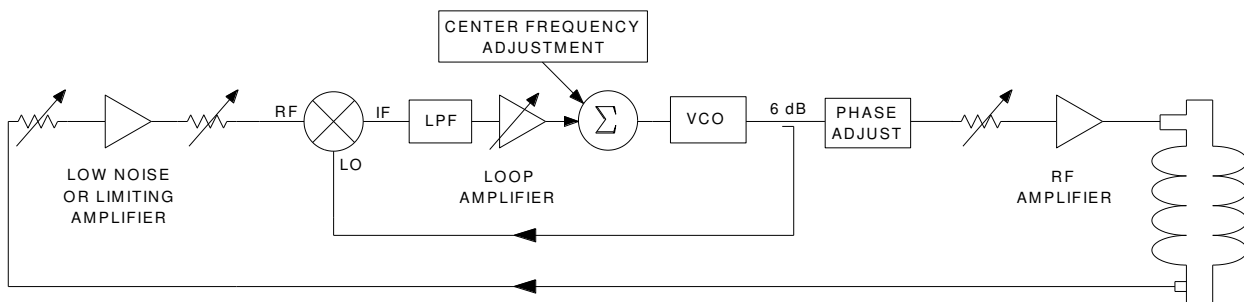

Figure 1: Block diagram of a typical VCO-PLL system which includes an RF amplifier and cavity structure.

amplifier, such as the difficult to find Lucent LG1605, provides an expanded dynamic range with reduced oscillation problems.

The LNA section is followed by a mixer. Typically double balanced diode ring mixers are used. Devices such as a Mini-Circuits ZFM-150 are perfectly adequate. The two major considerations are that the intermediate frequency (IF) output must be DC coupled and the operating level of the local oscillator (LO) should be as high as practical. Typically 7 to 13 dBm mixers are used. Mixers with a LO much higher than 13 dBm will require that one insert an amplifier between the coupled VCO output and the LO input.

The low pass filter (LPF) stage serves two purposes. The first is to eliminate any the frequency content at the fundamental frequency or it's second harmonic. The other purpose is to limit the loop bandwidth to about 20 kHz which reduces the system noise without compromising the lock time necessary for cavities which happen to have rise times on the order of 1 ms or less.

The variable gain amplifier provides another way to adjust loop gain that, unlike the LNA, is independent of loop phase. Unless the following phase shifter is capable of more than 360º of phase shift, this amplifier should have an invert switch. At the summing junction, the error signal is summed with an offset signal, that is typically generated using two ten-turn potentiometers, one for coarse and one for fine frequency adjustments. The reference voltage for the potentiometer is typically a band gap voltage reference based circuit. This is done in order to ensure that the source is stable and low noise. In addition to custom circuit designs, devices like a Stanford Research SR540 amplifier can be used to implement the loop gain and filter functions.

There are a number of choices for VCOs. The least expensive devices are broadband devices such as those produced by Mini-Circuits. While they have the advantage of low cost, they typically have electrical tuning ranges between 500 MHz and 1000 MHz. With a control voltage range between 10 and 25 Volts, these devices have a tuning a sensitivity, between 30 MHz/V and 100 MHz/V. Additionally, inexpensive devices are not thermally stabilized and are subject to thermal drifts. When excessive, these thermal drifts have been known to cause a cavity – VCO-PLL system to lose lock within minutes of being properly tuned. Such drifts can be mitigated by packaging the devices in a thermally isolated enclosure such as a foam lined metal box.

For a few thousand dollars one can purchase a custom VCO that is thermally stabilized. Devices manufactured by EMF Systems Inc., as well as others, can be mechanically tuned over a range of a few hundred MHz with an electrical tuning range and sensitivity on the order of 10 MHz and 1 MHz/V respectively. [7] (Note: Tuning sensitivities and ranges are given for VCOs operated between 800 MHz and 2 GHz.)

Although expensive, an excellent alternative for the VCO is to use an RF signal source that has an option for an external frequency modulation (FM) control which can be DC-coupled. Sources such as an Agilent E4422B work well for this application. This and similar RF sources have a low FM bandwidth, have stable low noise RF drive capabilities, and are flexible with respect to the operating frequency. They have an added advantage in that the output can be AM modulated simultaneous with FM modulation. This configuration is used when performing a measurement of the dynamic Lorentz force effects [5]. Remember when performing such tests that the minimum RF amplitude must be maintained at the LO port on the mixer for the system to function properly.

The final low level section consists of a directional coupler, along with the amplitude and phase controls. The directional coupler is used to provide the LO signal from the VCO to the input of the mixer. The specific coupling is determined by the output capability of the VCO and the required LO signal level. In some cases an amplifier must be used between the coupler and the mixer in order to provide sufficient signal level. Typically the phase shifter is a mechanical device such as a Narda 3752 or Arra D3428B. When selecting these devices insure that they provide at least 190º of phase shift or 370º depending on the configuration of the loop amplifier. For manual systems, a series of mechanical attenuators are used to adjust the RF drive level.

Figure 2 shows the phase shift for two such devices. Although called an attenuator, the ARRA device is a continuously adjustable variable coupler while the Narda attenuator is a switchable attenuator with 1 dB switching increments. Both of these devices would function well in a VCO-PLL system that is used for cavity testing. If not designed to be relatively phase stable such devices can have phase shifts on the order of 180º over a 20 dB range.
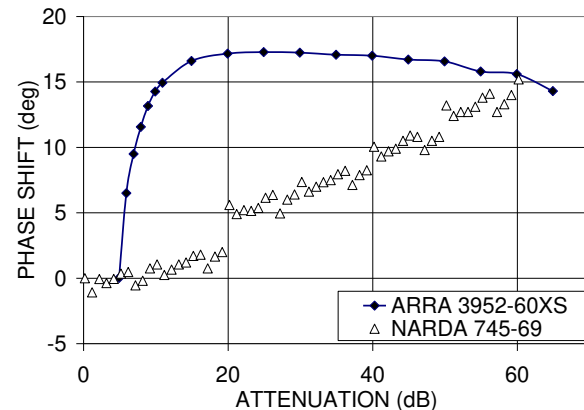

Figure 2: Phase shift as a function of attenuation for two different mechanical attenuators.

When one automates these systems, the first choice might be a PIN attenuator for this function. However, the phase of a PIN attenuator circuit shifts by about 60º when the attenuation is increased from 2 dB to 30 dB. A better choice is a vector, or I/Q, modulator. These devices work by splitting the RF into two components, known as in-phase (I) and quadrature (Q). The amplitude of the I and Q components are then varied as necessary; and recombined to provide independent control of phase and

amplitude of the RF. Discrete device I/Q modulators which use analog voltage controls are produced by companies like Analog Devices and Aligent Technologies. Connectorized devices with digital controls are available from GT Microwave and Vectronics, Inc.

The RF amplifier shown in the diagram varies depending on the loaded-Q of the cavity. For systems that are near critical coupling, i. e. very little reflected power at the input coupler, the amplifiers are usually solid state devices typically on the order of a few hundred watts. When the cavity is configured in a cryomodule they are typically strongly over coupled and the amplifier is typically a klystron delivering several kilowatts to several hundred kilowatts of RF power.

VERTICAL TEST SYSTEM

Figure 3 is a block diagram of a complete LLRF system used for testing cavities in the JLAB vertical test area. There are four basic blocks in the system. These are the transmitted power network, the power meter interface circuit, the VCO-PLL network and the amplitude and phase control network. It is an automated system that can be operated in manual mode. The computer controlled devices are augmented by devices that can be manually controlled.

Transmitted Power Networks

The RF signal produced by the cavity field probe is also called the transmitted power, P_T. Depending on the field probe-Q, it can range from tens of microwatts to several hundred milliwatts. The 3 dB attenuator shown in Figure 3 is used in order to limit the LNA drive signal at the

expected maximum transmitted power. The directional coupler is used to sample the transmitted power and provide it to the power measurement network. The two circulators ensure that the VSWR at the input circuits are minimized so that the calibration errors due to mismatch are minimized for the transmitted power metering circuit.

The combination of the two RF-switches, the PIN attenuator and amplifier provide gain control that is used to ensure that the crystal detector and mixer in the VCO-PLL circuit are neither over driven or power starved. The 6 dB attenuator was selected so that there is a minimum deadband as the amplifier used in this example has gain of 37 dB and the PIN attenuator has a 26 dB range. Thus there is a 5 dB deadband which is accounted for in the gain control software algorithm. The control interface allows one to either use computer control or manual control for selecting the status of switches SW1 and SW2 as well as the PIN attenuator setting. When computer controlled, the phase offsets of the PIN attenuator and the amplifier, are imbedded in the algorithm as a lookup table. The range of these values can be substantial. For example, the combination of the amplifier, switches and cables introduces a fixed 71º phase shift while the phase shift of the PIN attenuator varies by 62º range when the attenuation is adjusted from 4 dB to 32 dB. While the former could be minimized by adding a short section of cable into one leg of the system the latter is an intrinsic property of the device.

VCO-PLL

The VCO-PLL section is similar to that described earlier. In this case the VCO was moved to an external
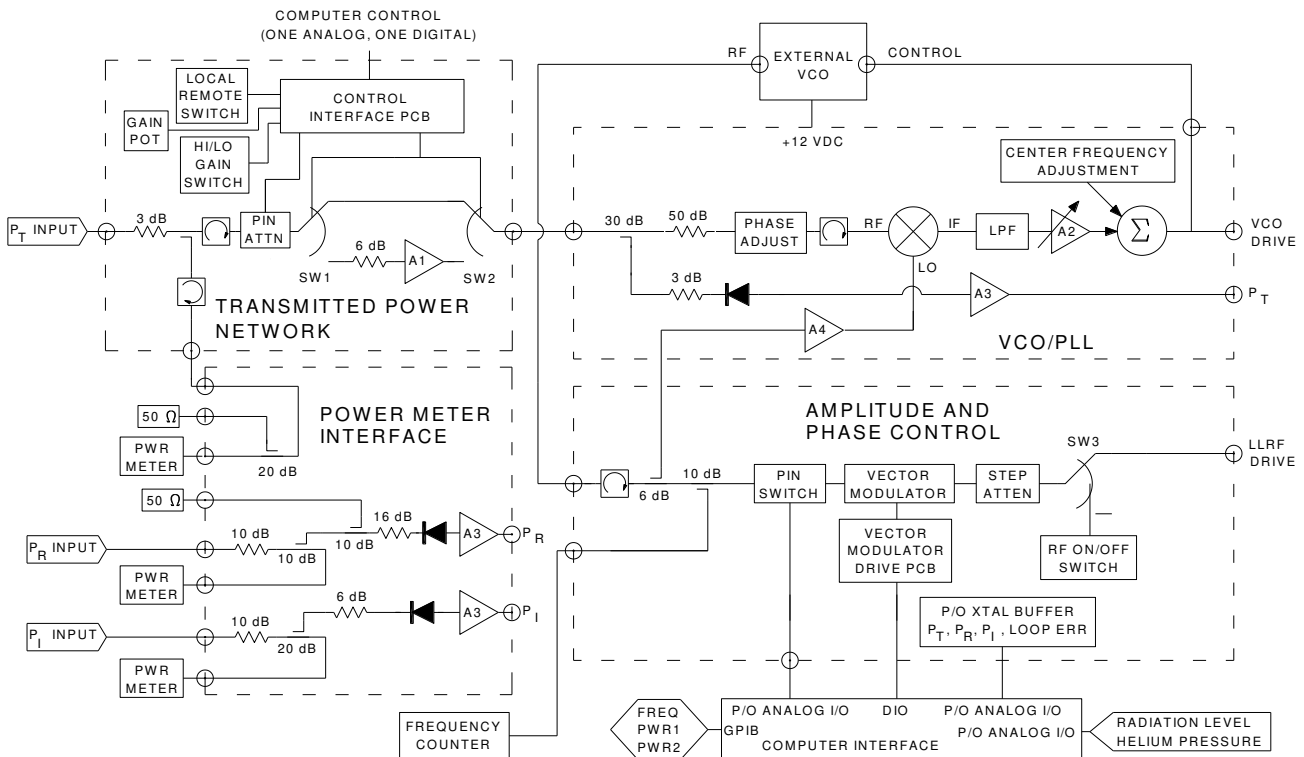

Figure 3: Block diagram of a typical low level RF system used for cavity testing.

location so that it could be thermally stabilized. Additionally, having it external allows one to use an alternate VCO for different applications. The 3 dB and 50 dB attenuators are carefully selected as part of the system optimization. The 50 dB attenuator is a major contributor to setting the loop gain. In this case the VCO is a broad band device with a sensitivity of about 5.6 MHz/V, thus the high value of attenuation. As a rule of thumb, the attenuator should be chosen to be 10 dB greater than the value at which the phase loop just starts to oscillate, but still low enough that the loop will lock and have a moderate lock range.

The 3 dB attenuator and the 30 dB coupler were chosen such that the crystal detector is not power starved and is still in the square law range when the loop is locked and not oscillating. While the incident and reflected power crystal detectors may be operated beyond the square law range without compromising the measurements, one must be careful to ensure that the transmitted power crystal detector is operated in the square law range, (i.e. between 10 and 25 mV at the output, depending on the detector and load combination) when making a decay measurement. As a matter of convenience and in order to ensure that there is adequate voltage available at the inputs to the data acquisition card in the computer, the gain of the A3-amplifiers was set to 400. Front panel connections provide an easy means to observe these signals using an oscilloscope. The A4 amplifier may be necessary depending on the output level of the VCO and the input requirements of the LO port on the mixer. In most instances it is not necessary.

Amplitude and Phase Control

The output of the VCO is routed to the amplitude and phase control section. The first device in that section is a circulator. It is there to ensure that frequency pulling due to impedance mismatches is minimized. Directional couplers are placed in the circuit to couple power out for the mixer local oscillator and the frequency counter. In this way both devices always have a constant level signal independent of the state of the output switches or amplitude control circuits. The PIN switch provides a means to pulse the RF on and off using either a pulse generator or the computer controls. In addition to tuning overcoupled cavities and verifying if the cavity is over coupled or under coupled, this switch is used when making decay measurements. The PIN switch is followed by an I/Q modulator and a step attenuator that were described previously. In most instances, computer control is used and the step attenuator is not operated. The on-off switch is actually an RF-relay that provides an easy way for the operator to control the application of RF power. It also provides a means to manually pulse the system. This manual pulsed operation is frequently used in critically coupled test of SRF cavities where cavity time constants in excess of a few tenths of a second are not uncommon.

Power Meter Interface

The two critical considerations for the power meter interface are stability of the components and low VSWR in the power meter signal path. Neglecting either of these will lead to unnecessary errors in the measurements. In addition to the function of protecting the power heads from damage due to peak RF power levels, the attenuators act as matching devices which absorb any reflections due to VSWR missmatch before they have a chance to multiply. The crystal detectors are provided so that the signals can be observed with an oscilloscope. Typically the three traces that are observed are the transmitted power signal, the reflected power signal and the VCO drive signal. The auxiliary RF ports on the transmitted and reflected power signals are provided so that a spectrum analyzer may be used rather than the crystal detectors.

Interlocks

During vertical testing medium power amplifiers between 100 W and 500 W are used to drive the cavities. No cavity protection interlocks are used during these tests at Jefferson Lab. Each facility and test should be evaluated individually. Engineering and administrative controls have been implemented to mitigate the hazards associated with ionizing radiation produced by field emission. The two major engineering controls are lead, steel and concrete shielding surrounding six of the eight vertical dewars as well as a personnel safety system (PSS). The PSS interlocks have been implemented so as to not allow one to apply high power RF to a cavity unless the PSS system can confirm that the shield lid is closed and no radiation is detected by the general area monitors.
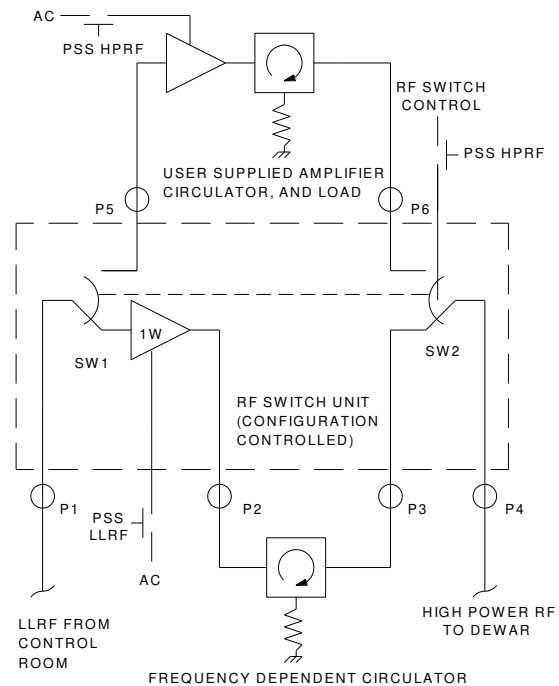

Figure 4: Block diagram of a typical RF interlock system used for vertically testing SRF cavities.

Figure 4 is a diagram of the research and development PSS interface. When the dewar lid is closed and high power operation is permitted, a contactor applies primary power to the amplifier and allows the operator to set the two RF-switches such that they route the drive signal to the user-supplied amplifier and output of that amplifier to the cavity. At other times the output of the one watt amplifier is routed to the cavity. This allows one to calibrate the system and do other low power tests while accessing the dewar top plate. The circulator used in the output of the low power amplifier is necessary to protect the amplifier from the emitted power pulse, which has peak power levels of several hundred watts. Such a pulse would be produced by the energy stored in the cavity if the PSS system were to change states while the cavity was in a high gradient state. A similar RF switching network, along with dewar selection switches and permanently installed cables was implemented for the Jefferson Lab cavity production systems.

CRYOMODULE TEST SYSTEM

Figure 5 is a block diagram of a complete RF system used at Jefferson Lab for testing cryomodules. The VCO-PLL used in this system is functionally the same as that used in the vertical test. It makes use of a vector modulator for amplitude and phase control. However, it still makes use of a mechanical phase shifter as it provides the operator with desired level of control.
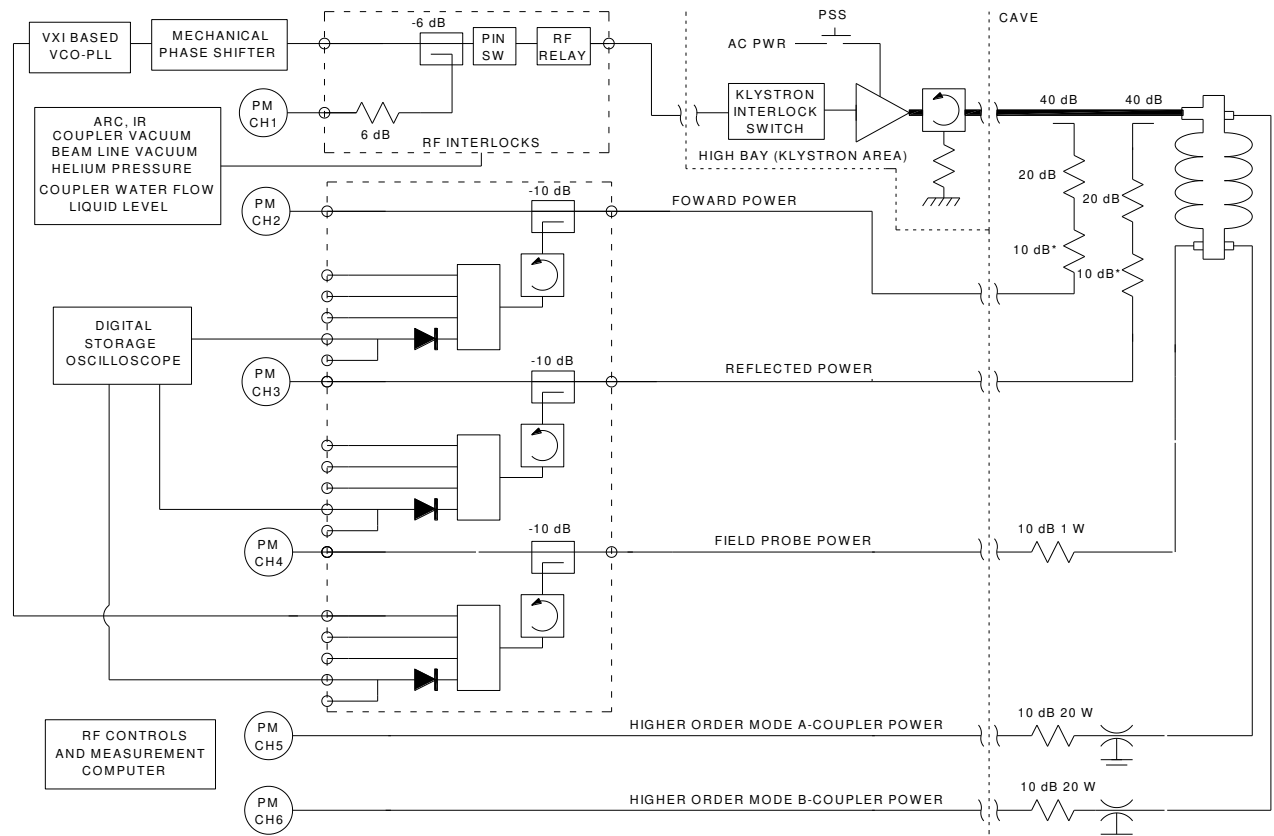
Interlocks

Unlike a cavity tested vertically, there is generally an excessive cost associated with recovery from damaging a cryomodule or failure of a high power coupler. In addition the much higher RF power available is capable of producing prompt damage. For these reasons, full interlocks are applied to the cryomodule when more than a few Watts of RF are applied to it. Typically, the interlocks used at Jefferson Lab include a subset of the following: coupler arc, both air side and vacuum side, infrared detectors for monitoring window temperatures, coupler vacuum, cavity vacuums, helium pressure, helium level, and coupler cooling water flow. When a fault in one of these interlocks occurs the LLRF drive signal is interrupted using both a PIN switch, for a fast reduction in applied RF power and an RF relay for a high isolation. The PSS system provides safety control by switching off the primary power feed to the klystron high voltage power supply in the event of an unsafe condition.

RF Measurement System

In this configuration, the core of the RF measurement system is a set of pulsed RF power meters. The meters that are used at Jefferson Lab are Boonton model 4532. They allowed us to acquire RF power waveforms that were linear to 2% at sample rates up to 2 MS/s. These devices were chosen for their ability to measure the emitted power and calculate the energy stored in the cavity during pulsed operation. The waveform records

Figure 5: Block diagram of a typical RF system used for cryomodule testing.

were transferred from the instruments and processed on a desktop computer in order to determine the cavity parameters.

The four way splitters were added to the system so that the RF signals could be used by other systems in parallel with the standard acquisition process. The crystal detectors were used for operator feedback. They were not calibrated and were frequently operated beyond the square law range. As in the VTA systems circulators and attenuators were distributed throughout the system in order to reduce the VSWR induced errors and to ensure that the power meter readings were not affected by changes in the configuration of the output ports on the 4-way splitters. Polyphaser B50 or MR50 series lightning arrestors were added to the HOM ports after several RF power heads and medium power attenuators, rated at 20 W(CW) and 500 W(peak), were destroyed during SNS cryomodule testing. Although precise measurements were not captured, excessive power was observed on a crystal detector when a cavity had a thermal quench. The leading hypothesis is that the frequency shift associated with a quench was more than several bandwidths of the HOM couplers notch reject filter. Thus power levels on the order of several tens of kilowatts was coupled out of the cavity for a few hundred microseconds.

At times during the SNS testing a 20 kW CW klystron was substituted for the 1 MW pulsed klystron. Iris plates and stub tuners were placed in the waveguide circuit just up stream of the fundamental power coupler, in order to increase the external-Q of the system. Administrative limits were put in place on the average cavity gradient when operating in this mode. The limit was set such that the equivalent average power rating of the coupler was not exceeded.

CONSTRUCTION TECHNIQUES AND AUTOMATION

There are two fundamental ways to build a cavity test system. An example of a research and development systems is shown in figure 6. Such a system has the advantage that it is extremely flexible and can be easily modified. The system shown is has all manual controls with cross coupling between phase and amplitude control. Generally, individuals who operate such systems must have a through understanding of the function and general characteristics of the different devices. The instrument readings are manually entered into a spread sheet where the different cavity parameters are calculated.

A chassis from a production system is shown in figure 7. Such a system is designed to be used by individuals who are skilled in the general operation of super-conducting cavities and have a basic understanding of the RF hardware but do not necessarily know all of the details regarding specific components used to build the LLRF system. Additionally, configuration control is important for production systems. Hardware that is imbedded in a chassis is more confidently stable and equally useful to multiple users.

Our production systems also make use of automation software. The software was written using LabView graphical programming language. Figure 8 is an example of a screen shot from the cryomodule test facility when

Figure 6: Example of a research and development system which is capable of being operated at frequencies between 500 MHz and 3 GHz.
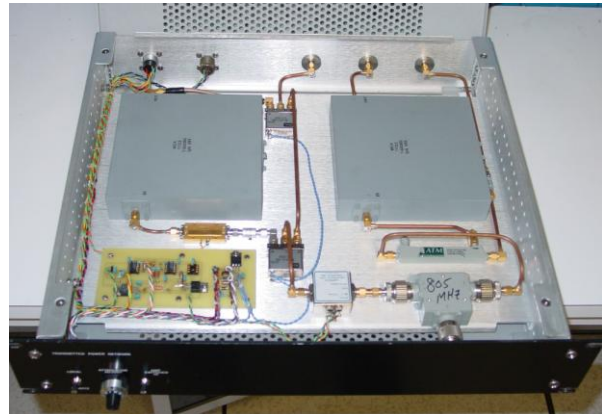

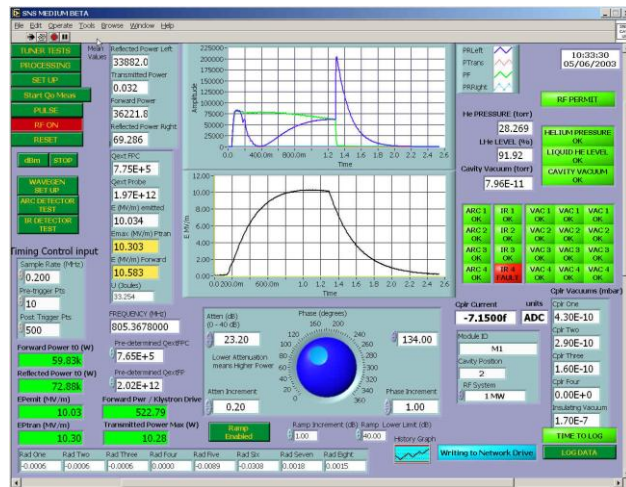Figure 7: Example of a chassis from a 500 MHz to 1 GHz production system..

Figure 8: Image of a screen of the cryomodule production software.

testing an SNS medium beta cavity. RF amplitude and phase are controlled by entering a value for attenuation and adjusting a phase knob. These values are combined and transformed into a pair of control voltages for a discrete I/Q modulator which is imbedded in a VXI-packaged VCO-PLL. Cable calibration values are entered into the program and the power meter readings are corrected in the software. The waveforms in the upper plot are of the reflected and forward power in Watts. When operated in a pulsed mode each set of acquired waveforms are processed to provide values for the relevant parameters such as peak power levels, average power levels, the stored energy at the end of the pulse, the external-Q of all of the cavity ports, etc. Once a careful measurement of the field probe external-Q is performed, the value is entered into the screen and the lower trace produces a time domain plot of the cavity gradient. Thus, the operator has constant feedback as to the operating point of the system. The software also has an interactive routine for making calorimetric Q_0 measurements. This software controls the heaters as well as the state (on-off) of the RF power. The routine also measures the rate of rise of the helium pressure and calculates the power dissipated by the cavity.

The vertical test software was written in a similar manner. One of the more useful features of this software is the interactive calibration routine with imbedded operator instructions. Again the software has controls for RF drive attenuation and phase controls which are transformed to I and Q values. It is capable of doing decay measurements in order to calculate the field probe external-Q. Once the field probe-Q has been established, a value is entered into the software and the operator has continuous feedback of the incident power, Q_0, cavity gradient, and field emission radiation levels. In both software packages the error in percent for the relevant variables is calculated and recorded to the data file as part of the process and displayed on the screens.

AUXILIARY EQUIPMENT

In addition to standard RF test equipment such as spectrum analyzers, network analyzers, low noise amplifiers, etc. we have found it useful when making microphonic measurements to have a dynamic signal analyzer, and a cavity resonance monitor. Another custom-made device that we used during production and testing of SNS couplers, is know as a vacuum conditioning controller. A similar device was used at CERN for conditioning the LEP power couplers [8]

Coupler Conditioning Controller

A simple diagram of a vacuum conditioning controller is shown in figure 9. As show, the system is capable of processing two couplers connected in series. Typically this connection is done through a rectangular waveguide structure. The waveguide on the output coupler can be either a fixed load or a sliding short [9]. The system uses the analog vacuum signals from the gauge controllers to control the klystron drive signal.

The difference between the set point and the actual each of the actual vacuum signals is multiplied by 2.5. These signals are diode added so that the larger of the two error signals is passed and eventually controls the RF power level. There is a gain adjustment and it as well as the set point, the raw vacuum signal, and the PIN-attenuator control voltage are monitored by a computer system
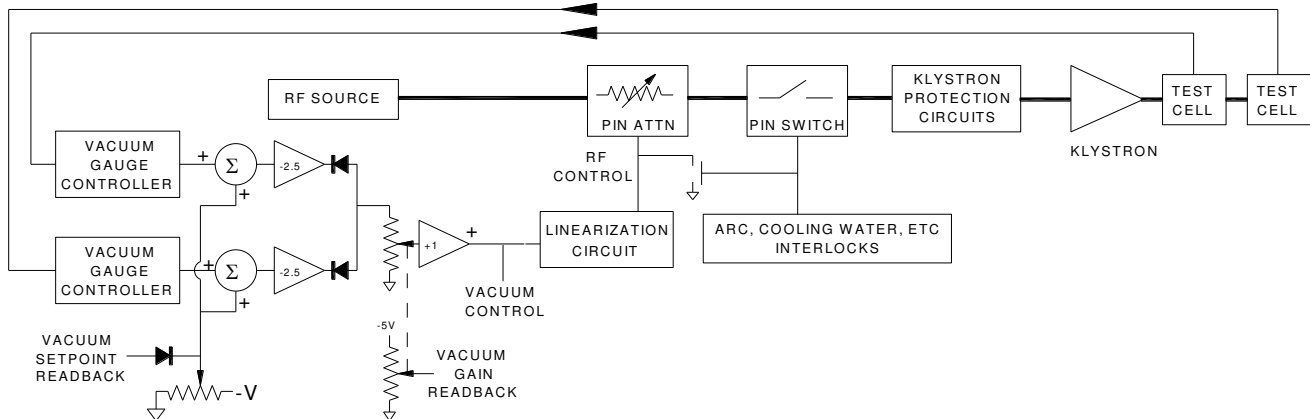

Figure 9: Block diagram of a vacuum conditioning system.

which has the capability of adjusting the RF source output. Redundant switching of the LLRF drive provides protection of the couplers in the event of an excessive vacuum excursion, cooling water faults, excessive heating or vacuum discharges. One millisecond response times have been measured with the limiting factor being the rise time of the analog output of the cold cathode gauge controllers. Although similar systems have been considered for operating cavities operated in a phase locked loop, the phase shift associated with the PIN attenuator has the potential to cause problems. Systems could be built that use fast digital controls such as an field programmable gate array or digital signal processor coupled with an I/Q modulator to control the RF drive signal with a minimum coupling between drive amplitude and phase shift.

Cavity Resonance Monitor

Cavity resonance monitors have been used for making frequency shift measurements on superconducting cavities for a number of years.[10] A schematic diagram of an analog cavity resonance monitor is shown in Figure 10. The circuit produces an output voltage that is proportional to the frequency difference between the input signal and a stable reference source. These devices are useful for characterizing the effect external vibration sources have on the operating frequency of superconducting cavities, measuring the transfer function of piezo and magneto-strictive tuners, and for measuring the ponderomotive effects due to dynamic Lorentz detuning effects.

The amplitude component, A, of the input signal given by:

$$A \cos \left(\omega_0 t + \varphi(t) \right) \qquad (1)$$

is removed by sending it through a limiter, with an output signal level that is within a 1% band, when the input signal is varied by 25 dB. If a limiter were not used the magnitude of the input signal would have to be measured and the output scaled by the input power level. The signal is split using a 90-degree hybrid to provide two signals:

$$i = \cos \left(\omega_0 t + \varphi(t) \right) \quad \text{and} \qquad (2)$$

$$q = \sin \left(\omega_0 t + \varphi(t) \right). \qquad (3)$$

With careful adjustment of the phase shifters, the LO signals on the two mixers have the same phase thus providing the following for the output of the mixers:

$$I = \cos \left(\omega_0 t + \varphi(t) \right) \cos(\omega_0 t) \qquad (4)$$

$$= \frac{1}{2} \cos \left(\varphi(t) \right) + \frac{1}{2} \cos \left(2\omega_0 t + \varphi(t) \right) \quad \text{and} \qquad (5)$$

$$Q = \sin \left(\omega_0 t + \varphi(t) \right) \cos(\omega_0 t) \qquad (6)$$

$$= \frac{1}{2} \sin \left(2\omega_0 t + \varphi(t) \right) - \frac{1}{2} \sin \left(\varphi(t) \right) \qquad (7)$$

Going to base band eliminates components of I and Q that contain $2\omega_0$ component. Taking the derivate of the two equations, multiplying, and summing the cross terms lead to the following:

$$I = \frac{1}{2} \cos \left(\varphi(t) \right) \rightarrow \frac{dI}{dt} = \frac{1}{2} \sin \left(\varphi(t) \right) \frac{d\varphi(t)}{dt} \qquad (8)$$

$$Q = \frac{1}{2} \sin \left(\varphi(t) \right) \rightarrow \frac{dQ}{dt} = -\frac{1}{2} \cos \left(\varphi(t) \right) \frac{d\varphi(t)}{dt} \qquad (9)$$

$$I \frac{dQ}{dt} + Q \frac{dI}{dt} = \frac{1}{4} \left[\cos^2 \left(\varphi(t) \right) + \sin^2 \left(\varphi(t) \right) \right] \frac{d\varphi(t)}{dt} \quad (10)$$

$$I \frac{dQ}{dt} + Q \frac{dI}{dt} = K \frac{d\varphi(t)}{dt} \qquad (11)$$

Where $d\varphi(t)/dt$ is equal to the change in cavity frequency as a function of time. The scaling factor, K, is calibrated by using two stable sources with a common reference signal. The frequency of one of the sources is varied while the difference in the output voltage is recorded. An alternate method when using a relatively stable cavity is to modulate the reference source slightly and measuring the change in the output signal.

When making dynamic microphonic or ponderomotive measurements one must be careful to avoid measuring the dynamic phase shift of the klystron. For instance, when using a pulsed RF system, droop in the klystron high
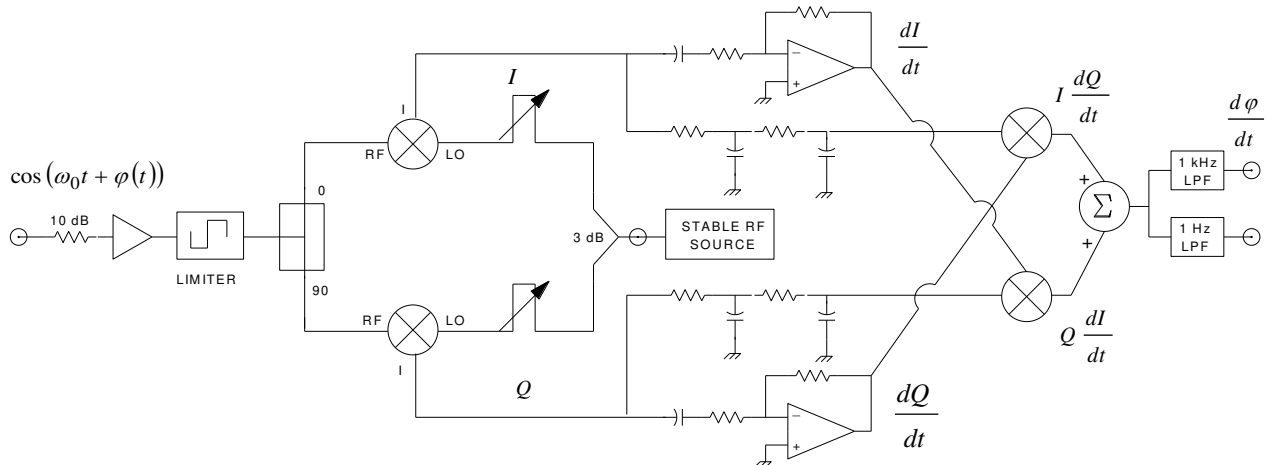

Figure 10: Block diagram of an analog cavity resonance monitor.

voltage supply can lead to substantial phase shift across the klystron. In such cases the VCO-PLL, which uses the VCO output as a reference signal, will track both the klystron and cavity phase shifts as a function of time. Thus when making dynamic transfer function measurements with a cavity resonance monitor, it is prudent to replace the LO drive signal on the mixer in the VCO-PLL with a sample of the klystron forward power signal.
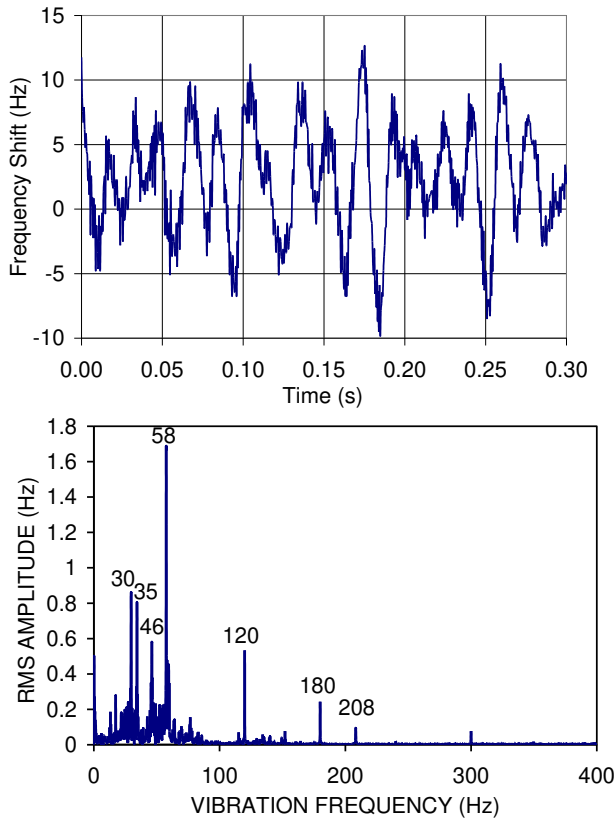

Figure 11: An example of background microphonic noise as measured with a cavity resonance monitor. The lower trace is an FFT of the time domain plot shown in the upper trace.

When building a cavity resonance monitor one must be very careful that the cutoff frequency for the integrator and low pass filters are precisely controlled and matched. If there is an offset between the frequency of the stable source and frequency being measure, the I and Q signals have a large magnitude component at that difference frequency. At higher difference frequencies, the second harmonic components of I and Q bleed through to the output giving false frequency components. A 5% mismatch in filter cutoff frequencies or gains will cause bleed through problems when the difference frequency is larger than 10% of the filter cutoff frequencies. During operation it is difficult to distinguish this bleed through signal from a driven microphonics signal.

A new DSP based system is currently under development at Jefferson Lab that shows a great deal of promise.[11] Using a CORDIC [12, 13] algorithm for phase determination and a high resolution analog-to-

digital converter eliminates the need for the need for the difficult to find limiting amplifier and simplifies the calibration processes. The system also eliminates the gain drifts issue as well as second harmonic bleed through issues.

CABLE CALIBRATIONS

The ability to do accurate, consistent cable calibrations is vital when testing cavities. Specific written procedures should be developed and verified as part of establishing a test program. Errors due to VSWR mismatch issues with the cabling, switching, etc. need to be quantified and included along with the calibration errors in the calculation of cavity parameters. When possible, cables should be calibrated using signal injection and measurement at the other end using either a source and power meter combination, or a network analyzer. Arithmetically, combining the calibration factor of individual components should be avoided if possible. In order to reduce VSWR induced errors, the components should be calibrated at or near the frequency of the test.

Calibration Procedure

Cable calibrations for cavity testing are complicated by the fact that one or more of the cables are only accessible from one end. In vertical tests the incident power cable the field prob cable as well as any higher order mode (HOM) coupler cables all have sections in the helium bath. In cryomodules tests all of these cables with the exception of the incident and reflected power also have one end within the vacuum vessel. The only way to measure the losses of a cable within a cryostat is to do a two loss measurement either with a calibrated network analyzer; or a source, a circulator and a power meter. The following are procedures used at Jefferson Lab for calibrating cables during a vertical test. See Figure 12 for the cable designations.

- To calibrate the cable from point A to point C. First, measure the one way loss of cable B-C.
  - Measure the reference source power level with the reference power meter. (P1)
  - Connect the reference source to point B of cable B-C.
  - Measure the power level with the transmitted power meter. (P2)
  - The one way loss is P1-P2 (dB)

- Measure the two way return loss of cable A-B
  - Connect the reference source to the input terminal of the circulator.
  - Connect the reference power meter to the load port on the circulator.
  - Record the reading on the reference power meter with the output port of the circulator open. (P3)
  - Connect the output port of the circulator to port B of cable A-B and record the reading on the reference power meter. (P4)

- The two way return loss of cable A-B is: $(P3 - P4)$.

- The cable calibration for the transmitted power meter, A-C path, is:

$$C_{AC} = \frac{(P1 - P2) + (P3 - P4)}{2} \text{ (dB)} \qquad (12)$$

- To calibrate the cable from point D to F and D to G Measure the forward power calibration from E to F
  - Connect the reference power meter to point E of the cable from the RF drive source.
  - Turn on the RF drive source and increase the power until the power level on the reference power meter is about 2/3 of the maximum allowed.
  - Record the power levels on the reference meter (P5) and the incident meter (P6)
- Measure the reflected power calibration from E to G
  - Turn off the RF source drive
  - Measure the reference source power level with the reference power meter. (P7)
  - Connect the reference source to point E of the path E-G.
  - Measure the power level with the reflected power meter. (P8)
- Measure the two way loss for the cable D-E with a slightly detuned cavity.
  - Connect the RF drive source to the cavity at point E.
  - Turn on the RF drive source and apply power to the cavity at a frequency about 10 to 20 kHz higher or lower than the cavity's resonant frequency.
  - Measure the incident (P9) and reflected power (P10) with the respective meters.
- The cable calibration for the incident, F-D path, and reflected power, G-D path, meters are:

$$C_{INC} = \frac{P5 - P6 + P7 - P8 - P9 + P10}{2} \text{ (dB)} \qquad (13)$$

$$C_{REFL} = \frac{P6 - P5 + 3 * P7 - 3 * P8 - P9 + P10}{2} \text{ (dB)} \qquad (14)$$

Calibration Verification

Two ways to verify calibration procedures are to calibrate the system using an external cable in place of the cable within the dewar then do one or both of the following. For the field probe cable calibration and reflected power calibration inject a known signal level into the external cable and measure the power using the calibrated power meter. For the forward power calibration connect the external cable to a remote power meter; inject a signal into the drive cable using the RF drive source; and measure the power using the remote power meter and the incident power meter. In both cases it can be a good exercise to vary the frequency over an 1 MHz to 2 MHz range and compare the values over the
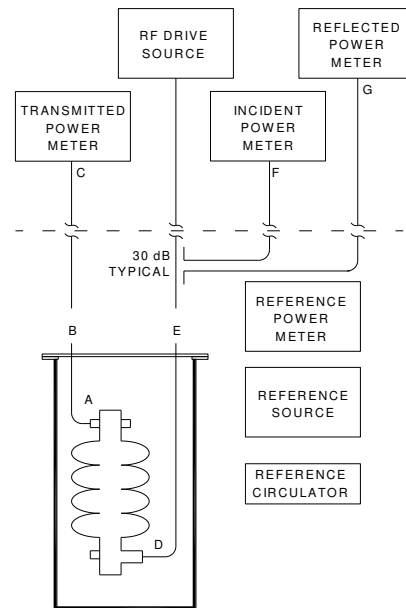

Figure 12: Diagram of the cabling and power meters used for a typical vertical test

range. Variations of more than a few percent the readings from the calibrated power meter and the reference power meter indicates excessive VSWR mismatches somewhere in the system.

A third way to verify the calibration and to look for VSWR problems in the incident power cable is to use the RF drive source to apply power to either an open test cable that has been calibrated or a detuned cavity. Record the values of the calibrated forward and reflected power as a function of frequency. They should be equal at all times. A variation in the difference between the two calibrated power measurements indicates a VSWR problem in the system. Figure 13 shows the results of such a measurement. The cabling with the minimal errors as a function of frequency made use of attenuators distributed throughout the signal path.
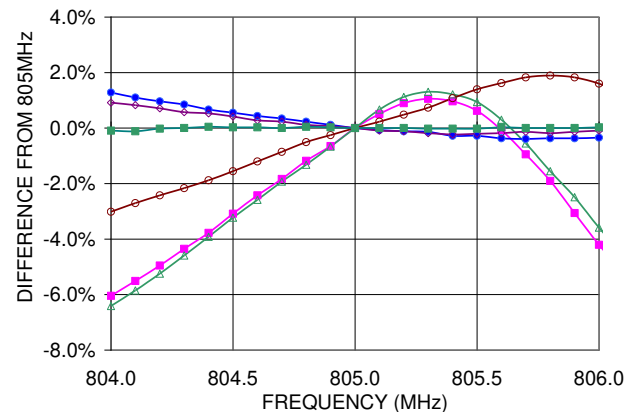

Figure 13: Difference between RF power measurements calibrated at 805 MHz and those taken at nearby frequencies for several different signal paths.

CABLE BREAKDOWN

When performing vertical tests at 2 K the incident power cables must pass through the low pressure helium gas in order to get to the fundamental power coupler.

The pressure at which helium goes superfluid is 35 Torr, and systems are typically operated at pressures between 20 and 25 Torr. Operating in this pressure regime with the typical dimensions of medium power RF connectors (i.e. 1 mm to 5 mm) means that the connectors are operating at or near the Pasching minimum of 4 Torr-cm. At this pressure-distance product the breakdown voltage in helium gas is minimized [14], and thus, there is a reasonable probability that glow discharges will occur. Work done by MacDonald and Brown in 1949 indicated that the minimum pressure for RF breakdown in helium was between 8 and 30 Torr depending on the geometery.[15] The probability of breakdown is further enhanced by field emission radiation. In general, this phenomenon is not new and has been extensively studied by individuals working in the satellite industry where it is known as multipactor breakdown. [16]

Observations

RF discharges have been observed in gas with as little as 10 W at 1500 MHz. Discharges have even occurred in connectors that were completely immersed in superfluid helium with incident power levels on the order of 150 W, full reflected, at the cavity. In all cases, discharges and the resulting damage have been observed in the volume within the connector space and in the connector back shell space. Both of these volumes do not contain dielectric materials.

Once a breakdown is initiated it will be sustained in superfluid helium by the forward power even at levels down to 10 W. The theory is that a few watts of heat is produced in the connector, possibly through thermal conduction down the insulated center conductor, from the antenna within the cavity, or in the connector pin itself. The liquid helium flashes to gas within the connector space and breakdown occurs within the newly produced low pressure gas volume. From the perspective of RF measurements, such events appear to be Q-switching within the cavity. The measured gradient appears to be reduced and the Q_0 as calculated using the dissipated power will be reduced substantially.

Determining if Breakdown Occurs

To determine if you have a cable discharge while it is occurring.

- Detune the frequency of the LLRF sytem far enough to lose lock in the VCO-PLL.
- Measure the forward and reflected power.
- Subtract the calibrated forward power from the calibrated reflected power to calculate the lost power.
- If any significant power is being lost, i.e. much beyond the errors in the measurements, you probably have a glow discharge in one of the connectors.

On occasion connectors damaged from this mechanism will exhibit this anomalous loss permanently at all power levels. Therefore, one should turn of the RF power and repeat the above steps at moderate power levels to ensure that the lost power is consistent with the error associated with the measurement.

System Improvements

The primary solution to the problem of cable breakdown is to never make RF connection rated for more that a few watts in low pressure helium gas. At Jefferson Lab we use silicon dioxide dielectric, stainless steel jacketed cables manufactured by Meggitt Safety Systems. The variant that we use has the outer conductor welded into a conflate flange. They make use of a hermetic fret to seal the exposed cable dielectric at connectors at each end of the cable. This ensures that the high power connections are only made in liquid helium and that there is no path for contaminating gas through the cable dielectric. Other solutions involve using epoxy to seal the outer jacket of the cable in a flange; building a secondary volume around the air side connection; and backfilling that space with helium gas so that any gas that leaks down the inner dielectric of the cable does not contaminate the helium system or to machine the outer conductor and dielectric off of the cable and epoxy it into the a metal sleeve as part of the feed through assembly.[17]

For the connections made in the helium bath, we also vent all connector volumes to the helium bath to improve the heat conduction of the space, especially the connector back shell space by drilling four holes, 3 mm in diameter in the outer conductor of the connector or back shell. Although improving the situation, connectors with this modification have been known to fail at power levels on the order of 200 W at the cavity when in a liquid helium bath. Another approach is to fill all potential spaces with an insulating material. In theory this should work but we have only had limited success at 200 W, 805 MHz forward power. One option that we have pursued but not fully implemented is to pressurize the cable with helium gas above the triple point of helium. This volume includes the connection to the vacuum feed through at the coupler antenna. Most important is to critically couple the cavities by carefully adjusting the input antenna or by using a variable coupler so that you do not have to use more than 150 W of RF power at the cavity.

FUNDAMENTAL EQUATIONS

During the cryomodule production cycle there are two basic types of high gradient RF tests that are done on cold cavities. In the first test the basic RF properties such as maximum accelerating gradient, field emission onset, and quality factor, Q_0, as a function of gradient are determined. At Jefferson Lab, as is done at many other labs, these tests are done in test cryostats where the cavities are held vertically. Ideally, these tests are done at or near critical coupling. In this way the RF source requirements are only a few hundred watts, which is just enough power to overcome the wall and field emission losses.

In the second type of test the cavities are installed in the final cryostat and they are typically strongly over coupled. This presents a problem as the errors in lost RF power get excessive when 95% to 99.9% of the incident power is reflected back out of the fundamental power coupler. Thus, during cryomodule tests the RF heat load is measured calorimetrically.

Table 1: Common variables used when discussing superconducting RF cavities.

Symbol	Variable Name	Units
r/Q	Geometric Shunt Impedance	Ω/m
G	Geometry Factor	Ω
E	Electric Field	V/m
L	Electrical Length	M
ω_0	Cavity Frequency	s^{-1}
U	Stored Energy	J
r_s	Surface Resistance	Ω
T_C	Critical Temperature	K
P_X	RF Power at Port X	W
P_{emit}	Emitted Power	W
R	Shunt Impedance	Ω
T	Operational Temperature	K
r_{resid}	Residual Surface Resistance	Ω
Q_0	Intrinsic Quality Factor	
Q_{FPC}	Fundamental Power Coupler Coupling Factor	
Q_{FP}, Q_2	Field Probe Coupling Factor	
R_C	Coupling Impedance	Ω/m
I	Beam Current	A
I_M	Matching Current	A
P_{disp}	Dissipated Power	W
τ	Decay Time	s
r	Shunt Impedance Per Unit Length	Ω/m

Summary of Variables Names and Units

Table 1 is a listing of the variables commonly used when discussing superconducting cavities, their names and associated units. The equations that follow were extracted from several sources over the years [18, 19, 20]. They are the basis for many of the RF measurements and associated calculations associated with SRF cavities. A good general reference for this material is entitled RF Superconductivity for Accelerators, by Padamsee, Knobloch and Hayes.

The Appendix of this document contains a complete set of equations used for making cavity measurements, near critical coupling using the decay method and the CW method as well as for making measurements of strongly over coupled systems. Additionally, the appendix contains equations used for calculating the errors associated with the calculated values.

The critical variable for calculating the RF parameters of a superconducting cavity is the shunt impedance, which relates the stored energy to the effective accelerating gradient, peak electric field, and peak magnetic field for any given mode. It is determined using electromagnetic simulation tools such as Mafia or Superfish. One should be careful in applying this variable as there are different definitions of shunt impedance, R, and geometric shunt impedance, (r/Q), in use[21]. For this paper, both variables are based on the definition that $R = V^2/P$, which includes the transient time factor.

General RF Measurement Equations

The following are general RF equations that apply to SRF cavities:

$$U = \frac{E^2}{\omega_0} \frac{L}{(r/Q)} \tag{15}$$

$$P = \frac{U\omega_0}{Q} = \frac{E^2}{Q} \frac{L}{(r/Q)} \tag{16}$$

$$Q_0 = G/r_S \| Q_{ElectronLoading} \tag{17}$$

$$r_S \approx 10 - 4(\Omega K/GHz\ 2)\frac{f^2}{T}e^{-1.95T_c/T} + r_{resid} \tag{18}$$

$$Q_L = Q_0 \| Q_{FPC} \| Q_{FP} \approx Q_{FPC} \tag{19}$$

$$R_C = Q_L(r/Q) \tag{20}$$

$$I_M = E/R_C \tag{22}$$

The power delivered to the beam is:

$$P_{Beam} = LEI \tag{23}$$

The coupling factor, β, is a measure of the efficiency of coupling RF power into the system it is given by:

$$\beta = \frac{1 - C_\beta \sqrt{P_{reflected}/P_{incident}}}{1 + C_\beta \sqrt{P_{reflected}/P_{incident}}} \tag{24}$$

where C_β is 1 for the under coupled and -1 for the over coupled case. For a cavity which are perfectly tuned and with the beam on crest, the power required by the klystron is:

$$P_{Kly} = \frac{(\beta + 1)}{4\beta} \frac{L(E + IR_C)^2}{R_C} \tag{25}$$

$$= \frac{(\beta + 1)}{4\beta} \frac{1}{Q_L} \frac{L}{(r/Q)} (E + IQ_L(r/Q))^2 \tag{26}$$

The Power reflected back to the circulator is:

$$P_{Ref} = \frac{(\beta + 1)}{4\beta} \frac{L(E - IR_C)^2}{R_C} \qquad (27)$$

$$= \frac{(\beta + 1)}{4\beta} \frac{1}{Q_L} \frac{L}{(r/Q)} (E - IQ_L(r/Q))^2 \qquad (28)$$

The time dependent complex differential equation where $\vec{K}$ is the incident wave amplitude in $\sqrt{Watts}$, ω_d is the (time varying) detune angle, and $\omega_f = \omega_0 / 2Q_L$:

$$\left(1\text{-}j\frac{\omega_d}{\omega_f}\right)\vec{E} + \frac{1}{\omega_f}\frac{d\vec{E}}{dt} = 2\vec{K}\sqrt{\frac{R_C}{L}} - R_C\vec{I} \qquad (29)$$

Adding microphonics and the effects of the difference cavity center frequency f_0 and that of the RF source, δf, and the beam current, I, being off crest by ψ_B leads to the equation (30) as the power required of the klystron.[20]

$$P_{Kly} = \frac{L}{R_C} \frac{(\beta+1)}{4\beta} \left\{ \begin{array}{l} (E + I_0 R_C \cos\psi_B)^2 \\ + \left(2Q_L \frac{\delta f}{f_0} E + I_0 R_C \sin\psi_B\right)^2 \end{array} \right\} \qquad (30)$$

When testing strongly overcoupled cavities $\beta \gg 1$, $Q_L \ll Q_0$ and $Q_L \ll Q_{FP}$ which means that $Q_L \approx Q_{FPC}$, in this case.

$$Q_L = 2\pi\tau \qquad (31)$$

$$E^2 = \frac{4\beta}{(1+\beta)} P_{Incident} Q_L \frac{(r/Q)}{L} \qquad (32)$$

Because $\beta \gg 1$, $\frac{4\beta}{1+\beta} \Rightarrow 4$ and, in this case.

$$E \approx \sqrt{4 P_{Incident} Q_L \frac{(r/Q)}{L}} \qquad (33)$$

Although using the above forward power to calculate gradient is a reasonable technique, practical experience says that there can easily be as much as 25% difference between the gradient as calculated using the forward technique power and the emitted power technique or using a well calibrated field probe. This difference can be reduced by properly tuning the phase locked loop, variable frequency system, or the cavity for a fixed frequency system.

Error Analysis

Most of the error analysis done when making cavity measurements can be done using a few fundamental equations as follows:

$$\frac{\Delta(AB)}{(AB)} = \sqrt{\left(\frac{\Delta A}{A}\right)^2 + \left(\frac{\Delta B}{B}\right)^2} \qquad (34)$$

$$\frac{\Delta(A+B)}{(A+B)} = \sqrt{\frac{\Delta A^2 + \Delta B^2}{(A+B)^2}} \qquad (35)$$

$$\frac{\Delta(\sqrt{A})}{(\sqrt{A})} = \frac{1}{2}\frac{\Delta A}{A} \qquad (36)$$

$$\frac{\Delta(AA)}{(AA)} = 2\frac{\Delta A}{A} \qquad (37)$$

The first two equations assume that the errors are Gaussian and uncorrelated. The factors of ½ and 2 found in equations (36) and (37) are because the errors are correlated. There are occasions, for instance the emitted power measurement, when using the simple equations is not appropriate and can lead to non causal errors. In such cases it is a simple matter to perform a Monte Carlo calculation to determine the dependencies. Additionally, care must be taken when chaining together calculations. For instance, determination of Q_{FP} for a strongly over coupled cavity includes any fixed calibration error in the transmitted power signal. If the calculated value of Q_{FP} is used to later calculate the gradient based on the transmitted power signal (using the same cable calibration factor), the error in the gradient should not include the transmitted power cable calibration factor. In this case the error in the transmitted power based gradient should only contain the error in the linearity of the power meter measurement and the error associated with Q_{FP}.

CRITICALLY COUPLED CAVITY MEASUREMENTS

When a cavity is near critical coupling, the process for determining the cavity parameters of E, Q_0, and Q_{FP} is as follows. The RF frequency and phase are controlled by a VCO-PLL. The phase is carefully adjusted to minimize the reflected power, which also maximizes the transmitted (i.e., the field probe) power. Then a decay measurement is made which determines the values of E, Q_0, and Q_{FP}. Once the results of the decay measurement is completed, Q_{FP} is used along with the RF power measurements to calculate E and Q_0.

The Decay Measurement

The decay measurement is initiated by pulsing RF power on and off so that one can determine if the cavity is over coupled or under coupled. Figure 14 shows the shape of the reflected power pulse for the different coupling conditions. Stable gradient is established and the steady state forward, reflected and transmitted power levels, (P_{Fwd}, P_{Ref}, and P_{Tran} respectively) are recorded. Next, the cavity drive signal is turned off and the decay time constant, τ, of the resulting transmitted power transient is determined using a crystal detector, a spectrum analyzer or a pulsed RF power meter.

The decay time, τ, is used to calculate a value for the loaded-Q, Q_L. Q_L, P_{Fwd}, P_{Ref}, and P_{Tran} are used to calculate Q_0. The gradient may then be calculated as:

$$E = \sqrt{P_{Loss} Q_0 \frac{(r/Q)}{L}} \qquad (38)$$

and the field probe-Q can be calculated as:

$$Q_{FP} = E^2 P_{Tran} \frac{L}{(r/Q)} \qquad (39)$$

As stated earlier, the operator must determine if the cavity is over coupled or under coupled prior to calculating the cavity parameters using the decay measurement technique. Typically a crystal detector is placed on the reflected power signal and the resultant signal is observed on an oscilloscope. Figure 14 is a depiction of the reflected power waveforms produced by a properly tuned cavity under different, near critical coupling, conditions.

In all of the reflected power pulses, the first peak has the same magnitude as the reflected power signal when the cavity is detuned. When the cavity is over coupled, the emitted power pulse, i.e. the second peak, is larger than the first peak. When the phase loop is properly tuned the minimum after the first peak goes through zero. When the cavity is critically coupled, the leading and trailing peaks are of equal magnitude and the reflected power goes to zero at the end of the pulse. When the cavity is under coupled the secondary peak, if there is one, is smaller than the first peak and the reflected power signal does not go to zero during the pulse.

OVER COUPLED $\beta > 1$

UNDER COUPLED $\beta < 1/3$

CRITICALLY COUPLED $\beta = 1$

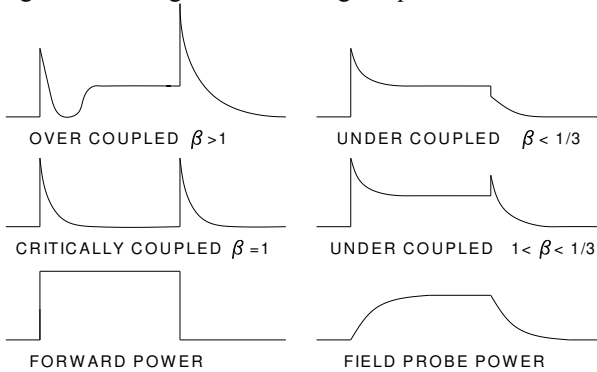UNDER COUPLED $1 < \beta < 1/3$

FORWARD POWER

FIELD PROBE POWER

Figure 14: Upper four traces are depictions of reflected power waveforms for various coupling states. The lower two traces are the corresponding forward and field probe pulse shapes.

CW Measurements

Once a value has been determined for the field probe-Q the calculations become much simpler. The gradient is given by:

$$E = \sqrt{P_{Trans} Q_{FP} \frac{(r/Q)}{L}} \qquad (40)$$

and the quality factor is given by:

$$Q_0 = E^2 P_{Loss} \frac{L}{(r/Q)} \qquad (41)$$

Decay Measurement Errors

Crystal detectors are frequently used to measure the decay time, τ. Other alternatives included using a pulsed RF power meter as discussed earlier or using a spectrum analyzer set up to do a zero span, time domain measurement. The crystal detector measurement relies on the fact that the crystal detector is operating within the square law range. In this power, or output voltage, range the output voltage is proportional to the RF power.

Using the half power, decay time constant technique, a properly terminated crystal detector can be used to make a +/- 3% measurement of the cavity decay time constant if the peak detector voltage is below 10 mV. If, for example, the same crystal detector were inadvertently used at 100 mV, the measured decay time would be overestimated by about 40%, the calculated Q_0 would be 40% higher than the actual value and the calculated cavity gradient would be 18% higher than the actual value.

Another source of decay measurement errors is changes in the loaded-Q during the decay measurement. Usually this is due to non linear effects such as field emission loading. As the energy stored in the cavity is emitted out of the fundamental power port, the gradient in the cavity is reduced; the field emission loading is reduced; and the loaded-Q is increased. This also occurs if the cavity has a strong Q-slope. The logarithmic slope of the decaying power is τ. In general τ is a function of E, or equalivently $Q_0(E)$. In such cases the decay slope at the start of the decay must be used, or a systematic error will lead to calculated Q_0 and E values that are larger than the actual values.

Lost Power Measurement Errors

Because the lost power is a difference between three power meter measurements, the error is given by the following:

$$\frac{\Delta P_{Loss}}{P_{Loss}} = \sqrt{\frac{\Delta P_{Fwd}^2 + \Delta P_{Ref}^2 + \Delta P_{Tran}^2}{\left(P_{Fwd} + P_{Ref} + P_{Tran}\right)^2}} \qquad (42)$$

Thus the error in the lost power increases dramatically when the reflected power approaches that of the forward power. Remember, when the cavity is critically coupled $\beta = 1$; the reflected power is equal to zero and virtually all of the forward power goes into wall heating. As $\beta = 1$ increases much above three or below one third the reflected power starts to become a substantial fraction of the wall heating power and the error in the lost power increases. This is the major contributor to the error is CW Q_0 measurements and decay measurement based of the gradient. Figure 15 are plots of the error in gradient and Q_0 as a function of β. The calculations assume that the power meter measurements, including cable calibrations are $\pm 7\%$, the linearity of the power meters is $\pm 2\%$, that τ is known to $\pm 3\%$ and that the power meters are operated well above their noise floor. Under these conditions, the error in the decay based gradient measurement and the CW Q_0 measurement vary because of the errors in the lost power calculation. Thus it is best to try to make all of the measurements when $0.5 \le \beta \le 2$.
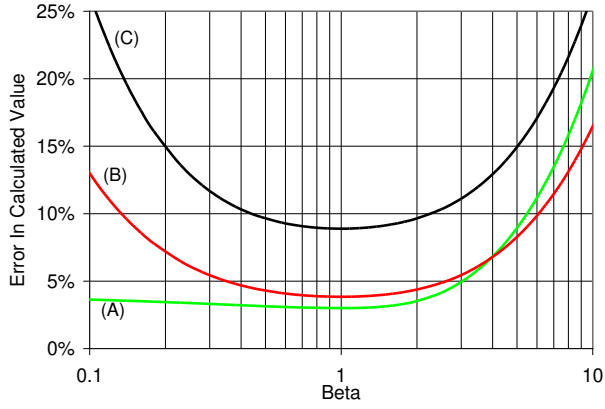
Figure 15 Error in (A) Q_0 as measured using a decay measurement, (B) E as measured using a decay measurement, and (C) Q_0 as measured using a CW measurement as a function of β.

STRONGLY OVER COUPLED CALCULATIONS

When a cavity is strongly over coupled the reflected power is approximately equal to the forward power. For example, a 5-cell CEBAF cavity, which has a frequency of 1.5 GHz and a loaded-Q of 6.6e+6, the value of β is 1500. Performing a decay measurement using the same techniques as described for critically coupled cavities would lead to errors in gradient and Q_0 that were on the order of 3000%. Other techniques must be used to characterize these cavities. The baseline measurement for the gradient is an emitted power measurement. The dynamic or RF heat load is usually made calorimetrically.

The emitted Power Measurement

Consider what happens when you suddenly remove the incident RF power from a cavity that has the stored energy U. This stored energy leaves the system through dissipation due to wall losses, i.e. Q_0 losses, and as RF power that is emitted from all of the RF ports in the system. Since $Q_L \ll Q_{FP}$ and $Q_L \ll Q_0$ in a strongly over coupled superconducting cavity the stored energy can be calculated as:

$$U = \int_{t_0}^{\infty} P_{emitted}(t)dt \approx \int_{t_0}^{\infty} P_{reflected}(t)dt \qquad (43)$$

Historically value of the stored energy was measured using a gating circuit and an RMS power meter [19]. In a sampled system, such as can be done with a Boonton 4532 pulsed power meter, the stored energy can be approximated by:

$$U \approx \sum_{m}^{N} \left(P_{reflected} \right) \Delta t \qquad (44)$$

Where m is the sample point where the incident power is removed and N is the total number of sample points. In addition to the errors associated with the power measurement, there are errors in this measurement which are introduced by the sampling system that can be reduced by proper choice of system parameters.

The uncertainty in the stored energy is given by the following:

$$\Delta U = \begin{cases} U \sqrt{\Delta C_R^2 + \Delta P_{CAL}^2} + \Delta t(N-m)C_R P_{min} \\ + (\Delta P_{emitted})_m \Delta t + \tau (P_{emitted})_N \end{cases} \qquad (45)$$

where ΔC_R is the percentage error in the power reading due to cable calibration errors; ΔP_{CAL} is the error in the power meter absolute calibration; and $\Delta g(N-m)C_R P_{min}$ is the contribution of the power meter noise floor during the integration. The next two terms are errors that, in most cases, can be minimized by setting up the acquisition window correctly. $(\Delta Penutted)_m \Delta t$ is due to start of the integration in the peak of the emitted power transient, see (A) in figure 14, and $\tau(Pemitted)_N$ is the error because the sum is to N and not to infinity, see (B) in figure 14. To reduce these errors one must sample at a high rate relative to the decay time and insure that $(m-N)\Delta t > 4\tau$.
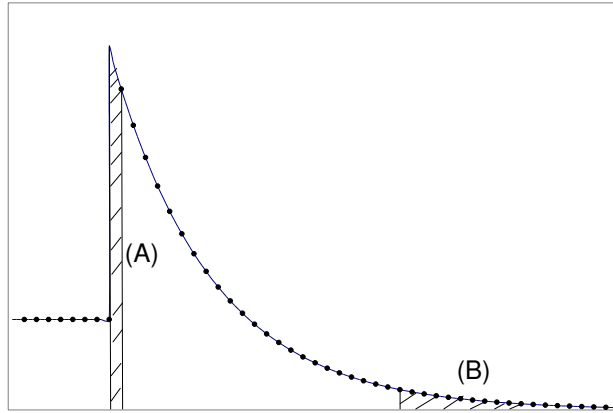

Figure 16: Depiction of two of the sources of errors that can occur when making an emitted power measurement digitally.

Once the stored energy has been determined the gradient can be calculated by using the following:

$$E_{Emitted} = \sqrt{2\pi f_0 * U * \frac{r/Q}{L}} \qquad (46)$$

where the Emitted subscript is just an indicator of the method used to determine the value. The field probe coupling factor, Q_{FP} can then be calculated using:

$$Q_{FP} = \frac{E_{Emitted}^2}{(P_{Transmitted})_{m-1}} * \frac{L}{r/Q} \qquad (47)$$

where $P_{Transmitted}$ is sampled just prior to removal of the incident power signal. Normally, an average of several points just prior to m is used for this value. One advantage of this technique is that the field probe calibration is accurate independent of how well the cavity was tuned or the shape of the incident power pulse. With good calibrations, proper sampling rates, and record

lengths, the gradient, E, can be measured with an accuracy of 5% to 7% and the *Q*-external of the field probe to about 10% to 12%.

Q_0 Measurements

In order to make a calorimetric measurement of the RF heating in a superconducting cavity, one must separate the static heat load from the RF heat load. A method that is used at Jefferson Lab is to measure the rate of rise of the helium pressure under different heat load conditions. During these tests the pressure is recorded for a fixed period of time, usually 30 seconds, and a linear curve fit is done in order to calculate the rate of rise. To perform this measurement.

- Close the inlet and outlet valves of the cryomodule and record the pressure as a function of time for 30 seconds.
- Apply a known amount of resistive heat to the bath and record the pressure as a function of time for 30 seconds.
- Turn off the resistive heater; tune the cavity; operated it at a fixed gradient and record the pressure as a function of time for 30 seconds.
- Turn off the RF power and record the pressure as a function of time for 30 seconds.
- Use the average of the static heat load measurements for the static rate of rise.

The dissipated power may be calculated as:

$$P_{RF\_HEAT} = \left| \frac{\left(\frac{dP}{dt}\right)_{RF-ON} - \left(\frac{dP}{dt}\right)_{STATIC}}{\left(\frac{dP}{dt}\right)_{HEATER-ON} - \left(\frac{dP}{dt}\right)_{STATIC}} \right| P_{HEATER} \quad (48)$$

where $\frac{dP}{dt}$ is the rate of rise of the pressure under the different conditions. Using the CEBAF style cryomodules which have a helium volume of approximately 1500 liters and a gas volume of about 50 liters, measurements with errors on the order of 0.5 W are possible. Thus this technique is not appliciable to low loss cavities at gradients much below 5 MV/m.

SUMMARY

Quality measurements necessary to qualify superconducting cavities require quality equipment designs, careful measurement techniques, and well characterized calibration processes. Specific equations for calculating the cavity RF parameters as well as the associated error for the parameters are included as an appendix. The errors are a function of the measurement equipment, the quality of the calibration and the specific conditions of each data point. As such, the error calculations should be included in the measurement system not as a part of post-processing the data. In systems where the cavity is near critical coupling, the error in a cavity gradient measurement can be reduced to 3% to 7%, and the Q_0 errors can be maintained below 10%. In strongly over coupled measurements the errors in the gradient can be reduced to 5% to 7%. However, the Q_0 measurements are limited to the minimum RF heat measurement accuracy of 0.5 W.

REFERENCES

[1] G. Davis, J. Delayen, M. Drury, E. Feldl, "Development and Testing of a Prototype Tuner for the CEBAF Upgrade Cryomodule," PAC 2001, pp 1149-1151.

[2] D. Barni, A. Bosotti, C. Pagani, R. Lange, H. Peters, "A New Tuner for TESLA", EPAC 2002, pp 2205-2207.

[3] G. Davis, J. Delayen, "Piezoelectric Tuner Compensation of Lorentz Detuning in Superconducting Cavities". PAC 2003, pp 1383-1385.

[4] D. Horan, E. Cherbak, "Fast Ferrite Tuner Operation on a 352 MHz Single-Cell RF Cavity at the Advanced Photon Source", PAC 2003, pp1177-1179.

[5] J. Delayen, G. Davis, "Microphonics and Lorentz Transfer Function Measurements on the SNS Cryomodules, SRF-2003, ThP21.

[6] A. Blanchard, Phase-Locked Loops, Application to Coherent Receiver Design, John Wiley & Sons, 1976.

[7] A. Ridenour, EMF Systems, Inc, State College PA, Personal Communication.

[8] H.K. Kindermann, M. Stirbet "RF power tests of LEP-2 main power couplers on a single cell superconducting cavity." 8th Workshop on RF superconductivity, Abano, Terme, Padua, Italy, 6-10 Oct 1997.

[9] M. Stirbet, K. Wilson, M. Wiseman, J. Henry, M. Drury, G. Davis, C. Grenoble, T. Powers, G. Myneni, I. Campisi, Y. Kang, D. Stout, RF Conditioning and Testing of Fundamental Power Couplers for SNS Superconducting Cavity Production. PAC 2005, to be published.

[10] G. Davis, J. Delayen, M. Drury, T. Hiatt, C. Hovater, T. Powers, J. Preble, "Microphonics Testing of the CEBAF Upgrade 7-Cell Cavity". PAC 2001, pp 1152-1154.

[11] T. Plawski, K. Davis, H. Dong, C. Hovater, J. Musson, T. Powers, "Digital Cavity Resonance Monitor-Alternative way to Measure Cavity Microphonics, 2005 SRF Workshop, to be published.

[12] J. Volder, "The CORDIC Trigonometric Computing Technique," IRF Transactions on Electronic Computers, V.EC-8. No. 3, pp 330-334.

[13] G. Griffin, "CORDIC FAQ", Lowegain's DSP Guru, http://www.dspguru.com/info/faqs/cordic.htm.

[14] J. Cobine, Gaseous Conductors Theory and Engineering Practices, Dover Publications, 1958.

[15] A. MacDonald, S. Brown, "High Frequency Gas Discharge Breakdown in Helium," Phys, Rev, V75. No. 1, Feb. 1, 1949, pp411-418.

[16] R. Woo, "Final Report on RF Voltage Breakdown In Coaxial Transmission Lines," NASA Technical Report 32-1500.

[17] A. Bosotti, G. Varisco, "A Reliable Coaxial Feedthrough To Avoid Breakdown in Vertical Test Facilities for SC Cavity Measurements", INFN Technical note INFN/TC-01/05.

[18] Padamsee, Knobloch, and Hays, RF Superconductivity for Accelerators, John Wiley & Sons 1998.

[19] I. Campisi, "Calibration of Cavity Field Probe", CEBAF-TN89-139.

[20] L. Merminga, J. Delayen, "On the Optimization of Qext Under Heavy Beam Loading and In the Presence of Microphonics," CEBAF-TN96-022.

[21] Padamsee, op. cit., pp47-48

ACKNOWLEDGEMENTS

Basic cavity formulas

r/Q	Geometric Shunt Impedance	Ω/m		T	Operational Temperature	K
G	Geometry Factor	Ω		R_{resid}	Residual Surface Resistance	Ω
E	Electric Field	V/m		$Q0$	Intrinsic Quality Factor	
L	Electrical Length	M		Q_{FPC}	FPC coupling Factor	
ω_0	Cavity Frequency	S^{-1}		Q_{FP}, Q_2	Field Probe Coupling Factor	
U	Stored Energy	J		R_C	Coupling Impedance	Ω
r_S	Surface Resistance	Ω		I	Beam Current	A
T_C	Critical Temperature	K		I_M	Matching Current	A
P_X	RF Power at Port X	W		P_{disp}	Dissipated Power	W
P_{emit}	Emitted Power	W		τ	Decay Time	s
R	Shunt Impedance	Ω		r	Shunt Impedance per Unit L	Ω/m

$$U = \frac{E^2 L}{(r/Q)\omega_0}$$

$$P = \frac{U\omega_0}{Q} = \frac{E^2 L}{Q(r/Q)}$$

$$Q_0 = G / r_S \| Q_{ElectronLoading}$$

$$r_S \approx 10 - 4(\Omega K / GHz^2)\frac{f^2}{T}e^{-1.95T_c/T} + r_{resid}$$

$$Q_L = Q_0 \| Q_{FPC} \| Q_{FP} \approx Q_{FPC}$$

$$R_C = Q_L(r/Q)$$

$$I_M = E / R_C$$

Power levels for strongly overcouple d cavites.

delivered to beam $\qquad LEI$

needed from the klystron $\qquad \dfrac{L(E + IR_C)^2}{4R_C} = \dfrac{1}{4Q_L}\dfrac{L}{(r/Q)}(E + IQ_L(r/Q))^2$

reflected to the circulator $\qquad \dfrac{L(E - IR_C)^2}{4R_C} = \dfrac{1}{4Q_L}\dfrac{L}{(r/Q)}(E - IQ_L(r/Q))^2$

Time dependent, complex diferentia l equation where $\vec{K}$ is the incident w ave amplitude in $\sqrt{\text{Watts}}$, ω_d is the (time varying) detune angle, and $\omega_f = \omega_0 / 2Q_L$:

$$\left(1 - j\frac{\omega_d}{\omega_f}\right)\vec{E} + \frac{1}{\omega_f}\frac{d\vec{E}}{dt} = 2\vec{K}\sqrt{\frac{R_C}{L}} - R_C\vec{I}$$

The equation for the power required for cavity center frequency f_0 detuned by δf and beam current, I_0, off crest by ψ_B :

$$P_{Klystron} = \frac{(\beta + 1)L}{4\beta Q_L (r/Q)}\left\{(E + I_0 R_C \cos\psi_B)^2 + \left(2Q_L\frac{\delta f}{f_0}E + I_0 R_C \sin\psi_B\right)^2\right\}$$

CEBAF Cryomodule testing RF Performance Characterization

Emitted Power Based Measurements

Starting Parameters:

$P_{im}, P_{rm}, P_{tm}, P_{ha}, P_{hb}$ − Actual Measured Power (Watts)

C_i, C_r, C_t, C_a, C_b − Cable Cal Factors relating measured Power to Associated Power at the Cavity

P_{emit} − Sampled Emitted Power - Value of the Reflected Power wit h no Applied Incident P ower.

$P_{disipated}$ − Disipated Power Mea sured Calimetric ally.

τ − Decay fit Parame ter for the $P_{Reflected}$ Signal Fit Starting at index point m

$r/Q \ (\Omega/m)$ − Cavity Shunt Impedance

$L \ (m)$ − Cavity Active Length

$U \ (J)$ − Cavity Stored Energy

$f_0 \ (Hz)$ − Cavity Res onant Freq uency

N - Data set sample size for pulsed measuremen t

m - Data Sample Set Index When the Incident P ower is Removed From the Cavity

k - Data Sample Set Index When the Incident P ower is Applied to the Cavity

Δt - Data sample interval.

T - Period of the pulsed waveform (Typically 60 Hz or less)

$E \ (V/m)$ - Cavity Gradient

$E_{(emit),(trans),(fpwr)} \ (V/m)$ - Cavity accelerati ng gradient as indicated by subscript

$Ports$ - number of RF ports on the cavity, includes beam pipes, HOM couplers, etc.

Derivation of Performance Parameters:

$$P_{incident} = P_{im} C_i$$

$$P_{reflected} = P_{rm} C_r$$

$$P_{transmitte \ d} = P_{tm} C_t$$

$$P_{hom \ a} = P_{ha} C_a$$

$$P_{hom \ b} = P_{hb} C_b$$

$$|\Gamma| = \sqrt{P_{reflected} \Big/ P_{incident}}$$

$$\beta = \frac{1 + |\Gamma|}{1 - |\Gamma|} \quad \text{(Overcouple d Cavity)}$$

$$Q_L = 2\pi f_0 \tau$$

CEBAF Cryomodule testing RF Performance Characterization

Emitted Power Based Measurements

$$U = \sum_{j=1}^{Ports} \left(\sum_{i=m}^{N} \left((P_{emit})_j \right)_i * \Delta t \right)$$

Where $(P_{emit})_j$ is the power emitted from the jth port on the cavity.

Assuming that $\{Q_0, Q_{extX}, \text{etc.}\} \gg Q_L$ or $P_{LOSS}, P_{tranX} \ll P_{emit}$

$$U \cong \sum_{i=m}^{N} (P_{emit})_i * \Delta t$$

$$E_{(emit)} = \sqrt{2\pi F * U * \frac{r/Q}{L}}$$

$$\Gamma = \sqrt{P_{reflected} \Big/ P_{incident}}$$

$$\beta = \frac{1+\Gamma}{1-\Gamma} \quad \text{Note}: \beta \gg 1 \text{ for strongly over coupled cavities}$$

For a perfectly tuned cavity :

$$E = \sqrt{\frac{4\beta}{(1+\beta)} * P_{incident} * Q_L * \frac{r/Q}{L}}$$

Assuming that $\beta \gg 1$ and that the cavity is perfectly tuned.

$$E_{(fpwr)} \cong \sqrt{4 P_{incident} * Q_L * \frac{r/Q}{L}}$$

$$Q_{tran} = \frac{2\pi f_0 * U}{P_{transmitted}}$$

$$Q_{hom\,a} = \frac{2\pi f_0 * U}{P_{hom\,a}}$$

$$Q_{hom\,b} = \frac{2\pi f_0 * U}{P_{hom\,b}}$$

$$E_{(trans)} = \sqrt{Q_{ext\,2} * P_{transmitted} * \frac{(r/Q)}{L}}$$

Assumes known value of $Q_{ext\,2}$ which is typically based on an emitted power measuremen t.

CEBAF Cryomodule testing RF Performance Characterization

Q0 Measurements

CW measurements where $P_{dissipated}$ is the average dissipated power measured calorimetrically.

$$Q_0 = \frac{E^2}{P_{dissipated}} * \frac{L}{r/Q} = \frac{2\pi f_0 * U}{P_{dissipated}}$$

For pulsed operation the gradient is not constant throughout the measurement. In this case the field probe transmitted power is recorded as a function of time with at a sample interval Δt; the gradient can be calculated using the transmitted power method; and Q0 is calculated as:

$$Qo = \frac{\frac{1}{T}\sum_{i=k}^{N} E^2_{(trans)i} * \Delta t}{P_{disapated}} * \frac{L}{r/Q}$$

Where $P_{dissipated}$ is the average dissipated power measured calorimetrically, and T is the period of the pulses. It should be noted that the numerator in the above equation is used to account for the non square pulse shape. Values of Q_0 calculated using this method will be different for different gradient pulse shapes or CW operations. If CW values are desired, it is best to make such measurements with pulse widths that are much greater than the cavity fill times.

To measure the dissipated power calorimetrically one isolates the cryomodule from the helium supply and return lines and records the rate of rise of the pressure under three conditions. These are static heat load with RF and resistive heaters on; static plus a known resistive heat load applied to the bath; and static plus a unknown RF heat load due to the cavity losses. The dissipated power is then calculated using the following.

$$P_{DISSIPATED} = \left| \frac{\left(\frac{dP}{dt}\right)_{RF-ON} - \left(\frac{dP}{dt}\right)_{STATIC}}{\left(\frac{dP}{dt}\right)_{HEATER-ON} - \left(\frac{dP}{dt}\right)_{STATIC}} \right| P_{HEATER}$$

where $\left(\frac{dP}{dt}\right)$ is the rate of rise of the pressure under the different conditions .

Derivation of Measurement Errors - Cryomodule:

Starting Parameters:

P_{min} − Sensitivit y limit of power sensors used

δP_{cal} − Fractional uncertaint y in absolute power measured

δC − Fraction al uncertaint y in cable calibratio ns

δP_{Lin} − Fractiona l uncertaint y of the linearity of the power meter measuremen t

Δ − Error of a variable . The units are the same as the variable, i.e. ΔP_{tran} is the error in P_{tran} in Watts.

Parameter Uncertainties:

$$\Delta P_{im} = P_{im} \times \delta P_{cal} + P_{min}$$

$$\Delta P_{rm} = P_{rm} \times \delta P_{cal} + P_{min}$$

$$\Delta P_{tm} = P_{tm} \times \delta P_{cal} + P_{min}$$

$$\Delta P_{ham} = P_{ham} \times \delta P_{cal} + P_{min}$$

$$\Delta P_{hbm} = P_{hbm} \times \delta P_{cal} + P_{min}$$

$$(\Delta P_{rm})_i = (P_{rm})_i \times \delta P_{cal} + mean \left(P_{min} \left|_{over\ 500\ pts}^{zero\ RF\ pwr} \right. \right)$$

$$\Delta P_{incident} = P_{incident} \sqrt{(\delta C)^2 + \left(\frac{\Delta P_{im}}{P_{im}} \right)^2}$$

$$\Delta P_{reflected} = P_{reflected} \sqrt{(\delta C)^2 + \left(\frac{\Delta P_{rm}}{P_{rm}} \right)^2}$$

$$\Delta P_{transmitte\ d} = P_{transmitte\ d} \sqrt{(\delta C)^2 + \left(\frac{\Delta P_{tm}}{P_{tm}} \right)^2}$$

$$\Delta P_{hom\ a} = P_{hom\ a} \sqrt{(\delta C)^2 + \left(\frac{\Delta P_{h\ am}}{P_{ham}} \right)^2}$$

$$\Delta P_{hom\ b} = P_{hom\ b} \sqrt{(\delta C)^2 + \left(\frac{\Delta P_{h\ bm}}{P_{hbm}} \right)^2}$$

$$(\Delta P_{emit})_i = (P_{reflected})_i \sqrt{(\delta C)^2 + \left(\frac{(\Delta P_{rm})_i}{(P_{rm})_i} \right)^2}$$

$$\Delta |\Gamma| = \frac{|\Gamma|}{2} \sqrt{\left(\frac{\Delta P_{reflected}}{P_{reflected}} \right)^2 + \left(\frac{\Delta P_{incident}}{P_{incident}} \right)^2}$$

$$\Delta U = U \sqrt{\Delta C_r^2 + \Delta P_{cal}^2} + (\Delta P_{emit})_m \, \Delta t + \tau \times P_N + \Delta t (N - m) C_r P_{min}$$

$\tau \times P_N$ term from not integratin g to ∞

$((P_{emit})_m \, \Delta t)$ Term is due to jitter for starting the integratio n

$\Delta t (N - m) C_r P_{min}$ Term is due to power meter noise floor

$$\Delta E_{emit} = \frac{E_{emit}}{2} \frac{\Delta U}{U}$$

$$\Delta E_{fpwr} = \frac{E_{fpwr}}{2} \sqrt{\left(\frac{\Delta Q_L}{Q_L} \right)^2 + \left(\frac{\Delta P_{incident}}{P_{incident}} \right)^2}$$

$$\Delta Q_{extX} = Q_{extX} \sqrt{4 * \left(\frac{\Delta E_{emit}}{E_{emit}} \right)^2 + \left(\frac{\Delta P_{transX}}{P_{transX}} \right)^2}$$

$$\Delta E_{transX} = \frac{E_{trans}}{2} \sqrt{\left(\frac{\Delta Q_{transX}}{Q_{transX}} \right)^2 + \left(\frac{\Delta P_{transX}}{P_{transX}} \right)^2}$$

Where Q_{trans} and ΔQ_{trans} were entered values that were determined under different operating conditions and calibrations than the current measurement.

$$\Delta E_{trans} = \frac{E_{trans}}{2} \sqrt{\left(\frac{\Delta Q_{trans}}{Q_{trans}} \right)^2 + \left(\frac{\Delta P_{Lin} * P_{transX} + C_X * P_{min}}{P_{trans}} \right)^2}$$

Where Q_{trans} and ΔQ_{trans} were determined under same operating conditions and calibrations than the current measurement.

$$\Delta Q_{0(fpwr)} = Q_{0(fpwr)} \sqrt{\left(\frac{2\Delta E_{fpwr}}{E_{fpwr}} \right)^2 + \left(\frac{\Delta P_{dissipated}}{P_{dissipated}} \right)^2}$$

$$\Delta Q_{0(trans)} = Q_{0(trans)} \sqrt{\left(\frac{2\Delta E_{trans}}{E_{trans}} \right)^2 + \left(\frac{\Delta P_{dissipated}}{P_{dissipated}} \right)^2}$$

$$\Delta \beta = \beta \sqrt{\left(\frac{\Delta |\Gamma|}{1 + |\Gamma|} \right)^2 + \left(\frac{\Delta |\Gamma|}{1 - |\Gamma|} \right)^2}$$

$$\Delta Q_L = Q_L \times \frac{\Delta \tau}{\tau} = Q_L \times \Delta P_{Lin}$$

CEBAF Vertical Pair Testing RF Performance Characterization

Decay Measurement Formulas

Starting Parameters:

$P_{im}, P_{rm}, P_{tm}, P_{ha}, P_{hb}$ − Actual measured CW RF power (Watts), just prior to turning the RF OFF for the decay measuremen t

C_i, C_r, C_t, C_a, C_b − Cable calibratio n factors relating measured RF power to associated RF power at the cavity.

C_β − Over/under coupling factor + 1 for under coupled, - 1 for over coupled.

τ − Decay fit darameter (seconds) for the emitted (as measured at the reflected power signal) or the transmitt ed power signal as measured when the incident R Fpower has been turne d OFF.

$f_0 (\text{Hz})$ − Cavity resonant frequency

Derivation of Performance Parameters:

$$P_{incident} = P_{im} C_i$$

$$P_{reflected} = P_{rm} C_r$$

$$P_{transmitte\ d} = P_{tm} C_t$$

$$P_{\text{hom}\ a} = P_{ha} C_a$$

$$P_{\text{hom}\ b} = P_{hb} C_b$$

$$P_{loss} = P_{incident} - P_{reflected} - P_{transmitte\ d} - P_{\text{hom}\ a} - P_{\text{hom}\ b}$$

$$|\Gamma| = \sqrt{P_{reflected} \Big/ P_{incident}}$$

$$\Gamma = C_\beta |\Gamma|$$

$$\beta^* = \frac{1 - \Gamma}{1 + \Gamma}$$

$$Q_L = 2\pi f_0 \tau$$

This implicitly assumes that Q_0 and the external-Q of all of the RF ports are independent of the stored energy, i.e. linear, flat Q_0, and constant coupling factor for gradients at or below that of the starting point of the decay measurement.

Decay Measurement Formulas Continued

$$Q^{*=} \frac{Q_L}{1 + \beta^*}$$

$$Q_1 = Q_0 / \beta_1$$

$$\beta_2 = P_{transmitted} / P_{loss}$$

$$\beta_3 = P_{hom\,a} / P_{loss}$$

$$\beta_4 = P_{hom\,b} / P_{loss}$$

$$\beta_1 = \beta^* (1 + \beta_2 + \beta_3 + \beta_4)$$

$$Q_0 = (1 + \beta_1 + \beta_2 + \beta_3 + \beta_4)Q_L$$

$$Q_2 = Q_0 / \beta_2$$

$$Q_3 = Q_0 / \beta_3$$

$$Q_4 = Q_0 / \beta_4$$

$$E_{acc} (V/m) = \sqrt{Q_0 P_{Loss} \frac{(r/Q)}{L}}$$

$$U (Joules) = \frac{Q_0 P_{Loss}}{2\pi f_0}$$

CW Formulas

Starting Parameters:

P_{im}, P_{rm}, P_{tm}, P_{ha}, P_{hb} – Actual Measured CW RF Power (Watts), just prior to turning the RF OFF for the decay measuremen t

C_i, C_r, C_t, C_a, C_b – Cable Calibratio n Factors relating measured RF power to associated RF power at the cavity.

C_β – Over/Under coupling factor + 1 for under coupled, - 1 for over coupled.

τ – Decay fit darameter (seconds) for the emitted (as measured at the reflected power signal) or the transmitt ed power signal as measured when the incident R Fpower has been turne d OFF.

Q_2 – Transmissi on Probe External Q as determined from a previous Decay measuremen t

f_0 (Hz) – Cavity Res onant Freq uency

Derivation of Performance Parameters:

$$P_{incident} = P_{im} C_i$$

$$P_{reflected} = P_{rm} C_r$$

$$P_{transmitte\ d} = P_{tm} C_t$$

$$P_{hom\ a} = P_{ha} C_a$$

$$P_{hom\ b} = P_{hb} C_b$$

$$P_{loss} = P_{incident} - P_{reflected} - P_{transmitte\ d} - P_{hom\ a} - P_{hom\ b}$$

$$|\Gamma| = \sqrt{\frac{P_{reflected}}{P_{incident}}}$$

$$\Gamma = C_\beta |\Gamma|$$

$$\beta^* = \frac{1 - \Gamma}{1 + \Gamma}$$

$$Q_0 = \frac{Q_2 P_{transmitte\ d}}{P_{loss}}$$

$$Q_1 = \frac{Q_0}{\beta_1}$$

$$Q_3 = \frac{Q_2 P_{transmitte\ d}}{P_{hom\ a}}$$

$$Q_4 = \frac{Q_2 P_{transmitte\ d}}{P_{hom\ b}}$$

CW Measurement Formulas Continued

$$\beta_2 = Q_0 \big/ Q_2$$

$$\beta_3 = Q_0 \big/ Q_3$$

$$\beta_4 = Q_0 \big/ Q_4$$

$$\beta_1 = \beta^* \left(1 + \beta_2 + \beta_3 + \beta_4\right)$$

$$Q_L = \frac{Q_0}{1 + \beta_1 + \beta_2 + \beta_3 + \beta_4}$$

$$E_{acc} = \sqrt{Q_2 P_{transmitte\,d} \frac{(r/Q)}{L}}$$

$$U(Joules) = \frac{Q_2 P_{transmitte\,d}}{2\pi f_0}$$

Derivation of Measurement Errors - Decay Measurement:

Starting Parameters:

$P_{im}, P_{rm}, P_{tm}, P_{ha}, P_{hb}$ - Actual Measured CW RF power meter reading (Watts), just prior to turning the RF off for the decay measurement.

P_{min} - Sensitivity limit of power sensor used.

δP_{cal} - Factional uncertainty in absolute power measured.

δP_{Lin} Fractional uncertainty in the linearity of the power meter calibration

δC - Fractional uncertainty in cable calibrations.

Δ - Error of a variable. The units are the same as the variable, i.e. ΔP_{tran} is the error in P_{tran} in Watts.

Parameter Uncertainties:

$$\Delta P_{im} = P_{im} \times \delta P_{cal} + P_{min}$$

$$\Delta P_{rm} = P_{rm} \times \delta P_{cal} + P_{min}$$

$$\Delta P_{tm} = P_{tm} \times \delta P_{cal} + P_{min}$$

$$\Delta P_{ham} = P_{ham} \times \delta P_{cal} + P_{min}$$

$$\Delta P_{hbm} = P_{hbm} \times \delta P_{cal} + P_{min}$$

$$\Delta P_{incident} = P_{incident} \sqrt{(\delta C)^2 + \left(\frac{\Delta P_{im}}{P_{im}} \right)^2}$$

$$\Delta P_{reflected} = P_{reflected} \sqrt{(\delta C)^2 + \left(\frac{\Delta P_{rm}}{P_{rm}} \right)^2}$$

$$\Delta P_{transmitte\,d} = P_{transmitte\,d} \sqrt{(\delta C)^2 + \left(\frac{\Delta P_{tm}}{P_{tm}} \right)^2}$$

$$\Delta P_{hom\,a} = P_{hom\,a} \sqrt{(\delta C)^2 + \left(\frac{\Delta P_{h\,am}}{P_{ham}} \right)^2}$$

$$\Delta P_{hom\,b} = P_{hom\,b} \sqrt{(\delta C)^2 + \left(\frac{\Delta P_{h\,bm}}{P_{hbm}} \right)^2}$$

$$\Delta P_{loss} = \sqrt{(\Delta P_{incident})^2 + (\Delta P_{reflected})^2 + (\Delta P_{hom\,a})^2 + (\Delta P_{hom\,b})^2 + (\Delta P_{transmitte\,d})^2}$$

$$\Delta |\Gamma| = \frac{|\Gamma|}{2} \sqrt{\left(\frac{\Delta P_{reflected}}{P_{reflected}} \right)^2 + \left(\frac{\Delta P_{incident}}{P_{incident}} \right)^2}$$

Derivation of Measurement Errors -   Decay Measurement Cont.:

$$\Delta\beta^* = \beta^* \sqrt{\left(\frac{\Delta|\Gamma|}{1+|\Gamma|}\right)^2 + \left(\frac{\Delta|\Gamma|}{1-|\Gamma|}\right)^2}$$

$$\Delta Q_L = Q_L \times \frac{\Delta\tau}{\tau}$$

$$\Delta Q^* = Q^* \sqrt{\left(\frac{\Delta\beta^*}{1+\beta^*}\right)^2 + \left(\frac{\Delta Q_L}{Q_L}\right)^2}$$

$$\Delta\beta_2 = \beta_2 \sqrt{\left(\frac{\Delta P_{transmitte\ d}}{P_{transmitte\ d}}\right)^2 + \left(\frac{\Delta P_{loss}}{P_{loss}}\right)^2}$$

$$\Delta\beta_3 = \beta_3 \sqrt{\left(\frac{\Delta P_{hom\ a}}{P_{hom\ a}}\right)^2 + \left(\frac{\Delta P_{loss}}{P_{loss}}\right)^2}$$

$$\Delta\beta_4 = \beta_4 \sqrt{\left(\frac{\Delta P_{hom\ b}}{P_{hom\ b}}\right)^2 + \left(\frac{\Delta P_{loss}}{P_{loss}}\right)^2}$$

$$\Delta\beta_1 = \beta_1 \sqrt{\left(\frac{\Delta\beta^*}{\beta^*}\right)^2 + \left(\frac{\Delta\beta_2^2 + \Delta\beta_3^2 + \Delta\beta_4^2}{(1+\beta_2+\beta_3+\beta_4)^2}\right)}$$

$$\Delta Q_0 = Q_0 \sqrt{\left(\frac{\Delta\beta_1^2 + \Delta\beta_2^2 + \Delta\beta_3^2 + \Delta\beta_4^2}{(1+\beta_1+\beta_2+\beta_3+\beta_4)^2}\right) + \left(\frac{\Delta Q_L}{Q_L}\right)^2}$$

$$\Delta Q_1 = Q_1 \sqrt{\left(\frac{\Delta Q_0}{Q_0}\right)^2 + \left(\frac{\Delta\beta_1}{\beta_1}\right)^2}$$

$$\Delta Q_2 = Q_2 \sqrt{\left(\frac{\Delta Q_0}{Q_0}\right)^2 + \left(\frac{\Delta\beta_2}{\beta_2}\right)^2}$$

$$\Delta E = \frac{E}{2} \sqrt{\left(\frac{\Delta Q_0}{Q_0}\right)^2 + \left(\frac{\Delta P_{loss}}{P_{loss}}\right)^2}$$

Derivation of Measurement Errors -   CW Measurement:

$P_{im}, P_{rm}, P_{tm}, P_{ha}, P_{hb}$ Actual Measured CW RF power meter reading (Watts).

P_{min} Sensitivity limit of power sensor used.

δP_{cal} Factional uncertainty in absolute power measured.

δP_{Lin} Fractional uncertainty in the linearity of the power meter calibration

δC Fractional uncertainty in cable calibrations.

Δ Error of a variable. The units are the same as the variable, i.e. ΔP_{tran} is the error in P_{tran} in Watts.

ΔQ_2 Uncertainty in Q_2 as determined from a decay measurement.

Parameter Uncertainties:

$$\Delta P_{im} = P_{im} \times \delta P_{cal} + P_{min}$$

$$\Delta P_{rm} = P_{rm} \times \delta P_{cal} + P_{min}$$

$$\Delta P_{tm} = P_{tm} \times \delta P_{cal} + P_{min}$$

$$\Delta P_{ham} = P_{ham} \times \delta P_{cal} + P_{min}$$

$$\Delta P_{hbm} = P_{hbm} \times \delta P_{cal} + P_{min}$$

$$\Delta P_{incident} = P_{incident} \sqrt{(\delta C)^2 + \left(\frac{\Delta P_{im}}{P_{im}} \right)^2}$$

$$\Delta P_{reflected} = P_{reflected} \sqrt{(\delta C)^2 + \left(\frac{\Delta P_{rm}}{P_{rm}} \right)^2}$$

$$\Delta P_{transmitte\,d} = P_{transmitte\,d} \sqrt{(\delta C)^2 + \left(\frac{\Delta P_{tm}}{P_{tm}} \right)^2}$$

$$\Delta P_{hom\,a} = P_{hom\,a} \sqrt{(\delta C)^2 + \left(\frac{\Delta P_{h\,am}}{P_{ham}} \right)^2}$$

$$\Delta P_{hom\,b} = P_{hom\,b} \sqrt{(\delta C)^2 + \left(\frac{\Delta P_{h\,bm}}{P_{hbm}} \right)^2}$$

$$\Delta P_{loss} = \sqrt{(\Delta P_{incident})^2 + (\Delta P_{reflected})^2 + (\Delta P_{hom\,a})^2 + (\Delta P_{hom\,b})^2 + (\Delta P_{transmitte\,d})^2}$$

$$\Delta |\Gamma| = \frac{|\Gamma|}{2} \sqrt{\left(\frac{\Delta P_{reflected}}{P_{reflected}} \right)^2 + \left(\frac{\Delta P_{incident}}{P_{incident}} \right)^2}$$

Derivation of Measurement Errors -   CW Measurement Cont.:

$$\Delta Q_0 = Q_0 \sqrt{\left(\frac{\Delta Q_2}{Q_2}\right)^2 + \delta P_{Lin}^{\,2} + \left(\frac{\Delta P_{loss}}{P_{loss}}\right)^2}$$

ΔQ_0 error assumes that the Q_2 used was measured using the same power meter and cable calibrations.

$$\Delta Q_0 = Q_0 \sqrt{\left(\frac{\Delta Q_2}{Q_2}\right)^2 + \left(\frac{\Delta P_{tran}}{P_{tran}}\right)^2 + \left(\frac{\Delta P_{loss}}{P_{loss}}\right)^2}$$

ΔQ_0 error assumes that the Q_2 used was measured using different power meter and cable calibrations.

$$\Delta Q_3 = Q_3 \sqrt{\left(\frac{\Delta Q_2}{Q_2}\right)^2 + \left(\frac{\Delta P_{hom\,a}}{P_{hom\,a}}\right)^2 + \left(\frac{\Delta P_{loss}}{P_{loss}}\right)^2}$$

$$\Delta Q_4 = Q_4 \sqrt{\left(\frac{\Delta Q_2}{Q_2}\right)^2 + \left(\frac{\Delta P_{hom\,b}}{P_{hom\,b}}\right)^2 + \left(\frac{\Delta P_{loss}}{P_{loss}}\right)^2}$$

$$\Delta \beta_2 = \beta_2 \sqrt{\left(\frac{\Delta Q_0}{Q_0}\right)^2 + \left(\frac{\Delta Q_2}{Q_2}\right)^2}$$

$$\Delta \beta_3 = \beta_3 \sqrt{\left(\frac{\Delta Q_0}{Q_0}\right)^2 + \left(\frac{\Delta Q_3}{Q_3}\right)^2}$$

$$\Delta \beta_4 = \beta_4 \sqrt{\left(\frac{\Delta Q_0}{Q_0}\right)^2 + \left(\frac{\Delta Q_4}{Q_4}\right)^2}$$

$$\Delta \beta^* = \beta^* \sqrt{\left(\frac{\Delta|\Gamma|}{1+|\Gamma|}\right)^2 + \left(\frac{\Delta|\Gamma|}{1-|\Gamma|}\right)^2}$$

$$\Delta \beta_1 = \beta_1 \sqrt{\left(\frac{\Delta \beta^*}{\beta^*}\right)^2 + \left(\frac{\Delta\beta_2^{\,2} + \Delta\beta_3^{\,2} + \Delta\beta_4^{\,2}}{(1+\beta_2+\beta_3+\beta_4)^2}\right)}$$

$$\Delta Q_1 = Q_1 \sqrt{\left(\frac{\Delta Q_0}{Q_0}\right)^2 + \left(\frac{\Delta \beta_1}{\beta_1}\right)^2}$$

$$\Delta Q_L = Q_L \sqrt{\left(\frac{\Delta Q_0}{Q_0}\right)^2 + \frac{\Delta\beta_1^{\,2} + \Delta\beta_2^{\,2} + \Delta\beta_3^{\,2} + \Delta\beta_4^{\,2}}{(1+\beta_1+\beta_2+\beta_3+\beta_4)^2}}$$

$$\Delta E = \frac{E}{2} \sqrt{\left(\frac{\Delta Q_2}{Q_2}\right)^2 + \left(\frac{\Delta P_{transmitte\,d}}{P_{transmitte\,d}}\right)^2}$$